Sven Fuest

Protective signalling mechanisms in the lung induced by open-lung ventilation strategies

Dissertation

lehmanns media

lehmanns media

Protective signalling mechanisms in the lung induced by open-lung ventilation strategies

Inauguraldissertation
zur Erlangung des Grades eines Doktors der Medizin
des Fachbereichs Medizin
der Justus-Liebig-Universität Gießen

vorgelegt von Sven Fuest
aus Münster

Gießen 2013

Bibliografische Information der Deutschen Nationalbibliothek
Die Deutsche Nationalbibliothek verzeichnet diese Publikation in der Deutschen Nationalbibliografie; detaillierte bibliografische Angaben sind im Internet unter http://dnb.ddb.de abrufbar.

Helmholtzstraße 2-9
10587 Berlin
Druck und Bindung: docupoint magdeburg, Barleben

ISBN 978-3-86541-610-0
www.lehmanns.de

Aus dem Zentrum für Innere Medizin
Medizinische Klinik und Poliklinik II
Universitätsklinikum Gießen und Marburg GmbH
Standort Gießen
Leiter: Prof. Dr. med. W. Seeger

Gutachter: Prof. Dr. W. Seeger
Gutachter: Prof. Dr. J. Schneider
Tag der Disputation: 20.11.2013

CONTENTS

1. INTRODUCTION

1.1. Architecture of the lung

The lung is a twin organ that is located in the chest, and is connected to the external environment by the trachea that divides into two principal *bronchi*. Further divisions generate the *bronchi lobares*, *bronchi segmentales*, *bronchioli*, *bronchioli terminales, bronchioli respiratorii, ductus alveolares* and alveoli. The alveoli are the locations for the gas exchange (99).

The alveoli are built from two types of epithelial cells, the type I pneumocytes and type II pneumocytes. The type I pneumocytes are responsible for gas exchange between the air in the alveoli and the blood in the capillary of the pulmonary vascular tree (52, 99). The alveolar type I cells cover approximately 95% of the alveolar surface (52). Further, the type I cells are part of the blood-gas barrier that separates the alveolar airspace from the interstitium (99). The type II pneumocytes cover approximately 5% of the alveolar surface and produce and secrete surfactant (52, 99). Another function of these cells is to clear fluid from the alveolus to prevent pulmonary oedema (52). Type II pneumocytes can also transform into type I pneumocytes (52, 99). Further, it is known that type II pneumocytes participate in immunologic reactions by producing cytokines and growth factors (52).

Another cell type involved in the generation of alveoli are interstitial pulmonary fibroblasts, which are responsible for the development and formation of the pulmonary extracellular matrix (ECM) (52).

Additional cell types that can be found in the lung are chondrocytes that are involved in the construction of the bronchial wall, adenocytes, so-called Clara cells in the wall of the *bronchioli terminales*, endothelial cells in the vessels, red blood cells and cells of the immune system (99).

1.2. Physiology of the lung

The function of the lung is to exchange gases by diffusion. That means the absorption of oxygen from the air and transmission to the blood, and transmission of CO_2 from the

blood to the alveoli with release of CO_2 into the air. For this, it is necessary that the air in the lung is regularly exchanged because gas diffusion is dependent upon a concentration gradient. The exchange of gas between the lung and the environment occurs by breathing. The airflow adjusts to volume changes of the lung.

The volume of the chest depends on the movement of the ribs and the diaphragm. The thoracic cavity is lined by the pleural sheets, where the *pleura visceralis* is linked to the lung and the *pleura parietalis* is linked to the ribs and the diaphragm. Because of a negative pressure between these sheets, thoracic expansion and contraction of the diaphragm lead to an increase in intrathoracic volume and an expansion of the lung with a negative pressure in the airways leading to a passive air flow into the lung. Decontraction of the diaphragm and descent of the ribs combined with the elastic retraction forces of the lung lead to a decrease in the volume of the thoracic cavity leading to air flow out of the lung. These dynamics can be illustrated with a pressure-volume curve [Figure 1; (106)].

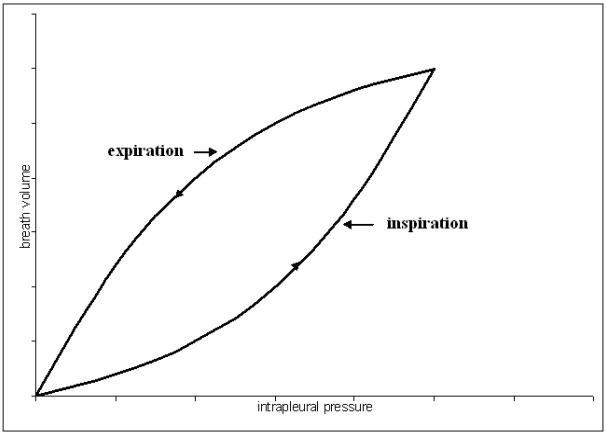

Figure 1: Pressure-volume curve in relaxed breathing. The intrapleural pressure - which translates to the intrathoracic cave - changes the intrapulmonary volume and the air flow. The intrapleural pressure is progressively negative from the left to the right. Modified from: (106).

Components that affect the gas exchange, apart from the gas concentrations in the blood and the air in the alveoli, are the surface area that participates in gas exchange, and the thickness of the alveolar septal wall that has to be transcended by the gases (106).

1.3. Acute respiratory distress syndrome

1.3.1. Pathophysiology

Acute respiratory distress syndrome (ARDS) is defined as a severe lung injury with acute onset, significant hypoxaemia, bilateral infiltrates on frontal chest radiography, and the absence of left ventricular failure (10, 36).

Hypoxaemia is measured by the PaO_2/FIO_2 ratio. That means the partial pressure of arterial oxygen related to the fraction of inspired oxygen. This ratio must be ≤300 for the diagnosis acute lung injury (ALI). Acute respiratory distress syndrome is the most severe subset of ALI with a PaO_2/FIO_2 ratio ≤200 (10, 36).

Symptoms of left ventricular failure can be dyspnoea, tachypnoea, cardiac asthma, basal rales, cyanosis, weakness, and cerebral dysfunction. The absence of left ventricular failure is equivalent to the absence of left atrial hypertension. The left atrial pressure can be assessed by the pulmonary capillary wedge pressure (PCWP). A PCWP of ≤18mmHg represents a normal left atrial pressure (51).

Lungs affected by acute respiratory distress syndrome exhibit morphologic and functional alterations in comparison with healthy lungs: the respiratory compliance is less, the dead space - parts of the lung that do not participate in gas exchange - is increased, and the partial pressure of arterial CO_2 is elevated (39).

The basis of ARDS is a direct or indirect pulmonary injury. Aspiration of gastric contents, pneumonia, inhalation of toxic gases, inhalation of hyperbaric O_2, intoxication with local applied narcotic drugs or lung transplantation can lead to a direct injury. Reasons for an indirect injury can be a sepsis, shock, lipid embolism, burns, intoxication with systemic applied drugs, and pathologic intravascular coagulation (50).

Irrespective of the aetiology, ARDS has three phases. The first is the exudative phase, the second the proliferative phase, and the third the fibrotic phase (35, 81, 109). The exudative phase takes up to six days and is characterised by hyaline membranes in the alveolar walls, oedema and inflammation (81, 109). The four to ten days of the proliferative phase are characterised by a metaplasia of pneumocytes with reduced production of surfactant and proliferation of myofibroblasts (35, 81). Lung fibrosis and pulmonary hypertension are the leading characteristics of the eight or more days that make up the fibrotic phase (81, 109).

The survival in ALI/ARDS depends on the age of the patient, accessory chronic diseases, and extra-pulmonary organ dysfunction (11).

Acute respiratory distress syndrome and ALI are common diseases with a significant socio-economic burden. The accurate incidence rates differ depending on the criteria used to diagnose ALI and ARDS in different studies, and depending on the selected population. For example, Luhr *et al.* found with the criteria of the American-European Consensus Conference [see above, (10)] incidence rates of 13.5 cases per 100,000 inhabitants per year for ARDS and 17.9 cases of ALI per 100,000 inhabitants per year for Sweden, Denmark and Iceland (62, 75). The 90 day mortality in this study was above 41% in ARDS and in ALI patients (75).

1.3.2. Animal models

Multiple animal models for ARDS exist. Pneumonia can be induced by intratracheal instillation of *E. coli*. Due to this infection, the inflammatory response in this model is higher than in non-infectious animal models (57). Another manner of inducing ARDS is the infusion of lipopolysaccharide (LPS) as a model for sepsis (58). In the LPS model, inflammation and haemorrhage play the crucial role in lung injury (58). By injection into the central venous vasculature, oleic acid arrives in the pulmonary vessels and leads to endothelial and epithelial necrosis in the lung (86). In this case, the lung develops oedema and atelectasis (57, 86). Another possibility to induce lung injury is the repeated lavage of the lung with saline, causing surfactant depletion (57, 58, 86). This model is applied as a model for neonatal respiratory distress syndrome and for early ALI in adults (57). Lachmann *et al.* developed the saline washout model for removing surfactant phospholipids from the alvoeli. This procedure causes collapse of unstable alveoli and subsequent conditions similar to ARDS (60). While the pneumonia model is chracterised by a gross inflammation, the oleic acid injection and saline lavage models induce lung injury by a reduction in respiratory system compliance and gas exchange (57). In both models the respiratory mechanics and the decreased gas exchange that lead to hypoxaemia are similar (73, 97). Beyond that, the oleic acid model is marked by a distinct oedema (86). Whereas two of these models (LPS, oleic acid) represent indirect lung injurious mechanisms, the pneumonia and the saline lavage models lead to a direct lung injury. The saline lavage model produces acute hypoxaemia where the animal is

haemodynamically stable (97). It is conceivable that the inflammatory response in the pneumonia model leads to a haemodynamic instability in terms of cardiovascular decompensation.

1.4. Ventilator-induced lung injury

1.4.1. Pathophysiology

Physiologically, breathing works because air flows into the lung due to a negative intra-thoracic pressure. Mechanical ventilation changes the mechanism by which air enters the lung.

Ventilator-induced lung injury (VILI) results from injurious mechanical ventilation. Mechanical ventilation is a method for oxygenation of patients who are not able to breathe by themselves or who are in danger of being unable to breathe by themselves. Therapeutic mechanical ventilation is used for central respiratory paralysis (e.g. during depression of the respiratory centre in the brainstem by drugs such as barbiturates or opioids; or because of damage to the respiratory centre by a trauma or a tumour), for peripheral respiratory paralysis (e.g. due to paraplegia or a muscle relaxant), for lung failure (e.g. because of oedema, pneumonia or pulmonary embolism), for disordered respiratory mechanics (e.g. by fractures of serial ribs or fracture of the sternum) and for an increase in respiratory resistance. Prophylactic mechanical ventilation is used on unconscious patients for preventing aspiration, on patients who have already aspirated, on patients with an extended shock, on patients with a sepsis, on patients with burns, for elevated intracranial pressure and for attenuating cardio-pulmonary stress (103).

Ventilator-induced lung injury includes barotrauma, volutrauma, atelectrauma, and biotrauma (43, 102). Barotrauma is associated with very high positive end-expiratory pressure (PEEP) of >40 cm H_2O and with peak inspiratory pressures (PIP) of >100 cm H_2O; but barotrauma does not seem to play an essential role in VILI (54, 102).

As Halbertsma *et al.* describe, the main determinant of volutrauma is the end-inspiratory volume (43). Volutrauma consists of diffuse alveolar damage, pulmonary oedema, an increase in fluid filtration, and loss of epithelium barrier (102). Dysfunction or inactivation of surfactant during mechanical ventilation may also participate in the development of oedema through a change in epithelial permeability due to an increase

of alveolar surface tension (34). Another reason for oedema appears to be the disruption of the blood-gas barrier, primarily in the endothelium due to loss of the endothelial cell contact to the basement membrane during injurious ventilation (118).

Cyclic opening and collapse of the alveoli during mechanical ventilation causes an increase in working stretch and shear forces resulting in lung injury [atelectrauma; (43, 102)]. Dreyfuss and Saumon speculate that at the beginning of the atelectrauma, surfactant inactivation leads to atelectasis with an augmentation of shear stress (34).

The fourth component of VILI - biotrauma - is due to an upregulation of cytokine production in the lung, causing an inflammation - mainly an immigration of neutrophils into the alveolar spaces (53) - and further injuring of the lung. Mechanical ventilation may lead to systemic inflammatory response syndrome (SIRS) and to multiple-system organ failure (MSOF), leading to death (33, 102).

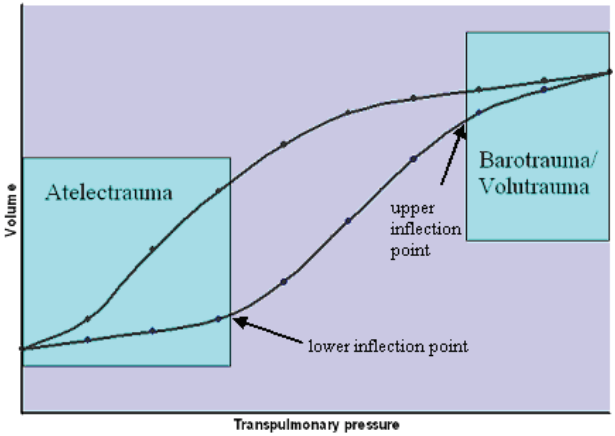

Figure 2: Effect of mechanical ventilation on a pressure-volume curve. The boxes mark the most susceptible ventilation conditions for the development of the designated components of VILI. The pressure increases from the left to the right. Modified from: (102).

Figure 2 illustrates regions in the pressure-volume curve that are associated with different components of VILI (102). The International Consensus Conference in Intensive Care Medicine identified volutrauma and atelectrauma as the two main determinants of VILI (54). The menace of atelectrauma is greatest during ventilation with pressures below the lower inflection point (96). The lower inflection point is

thought to represent the pressure/volume at which the alveoli are recruited (122). The risk of volutrauma is greatest using pressures above the upper inflection point (96). This upper inflection point marks the pressure/volume at which the alveoli are damaged due to overinflation (122).

The two most important cell types for the development of VILI seem to be alveolar macrophages and the pneumocytes (33). It has been shown that macrophages are responsible for an intense increase of interleukin (IL)-8 production due to mechanical stress (38). Macrophages also seem to play a crucial role in the mechanical stress-induced lung remodelling. Furthermore, high TNFα (tumour necrosis factor α) production seems to be dependent on macrophages (33). Another source of chemokines may be the alveolar epithelial cells that produce TNFα in response to injurious ventilation. Dos Santos and Slutsky postulate a crucial role for the pneumocytes as cytokine and chemokine producers in VILI because of the highly exposed position of the pneumocytes with respect to the mechanical stimuli during mechanical ventilation (33).

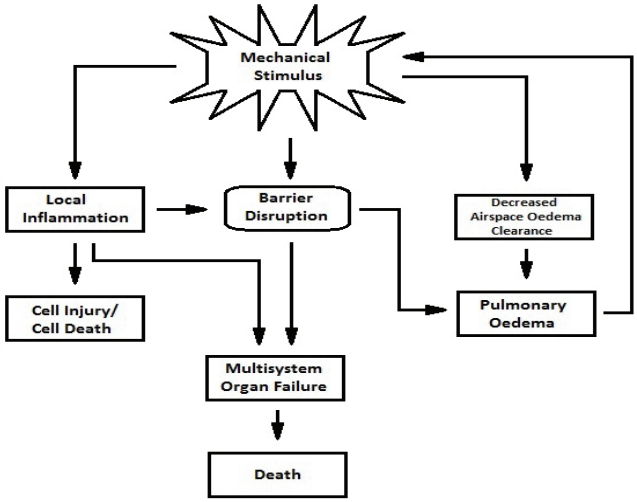

Figure 3: Overview of potential mechanisms of development and consequences of VILI. Modified from: (38).

It is hypothesised that there are reciprocal interactions between the biotrauma-related immunoreactions and mechanical stress leading to volutrauma, because microbial products such as LPS enhance responses due to mechanical ventilation, and mechanical stress aggravates this response to microbial products (78). Figure 3 provides an overview of potential mechanisms involved in VILI (38).

1.4.2. Lung protective ventilation

One lung protective ventilation management strategy (90) is known as the "open lung" concept that was coined by Lachmann. The components of this strategy are a pressure-controlled ventilation with an initial PIP of 40 – 60 cmH_2O (recruitment maneuver) that is adjusted individually due to recruitment, a ratio of the duration of inspiration to expiration (I:E) of 1:1 to 2:1, a PEEP of 10 – 20 cmH_2O, a permissive hypercapnia, and an initial inspired O_2 concentration of 100% that is reduced in long term ventilation to levels as less as tolerated by the patient. The fundamental idea is that terminal units are stabilised with an appropriate level of PEEP. This leads to an increase in the aerated lung fraction and may reduce regional overinflation so that VILI could be limited (54, 74). Further, PEEP may lessen the atelectrauma by stabilising the terminal units leading to less shear stress of the pneumocytes (34, 38, 90). This could be explained by preserved surfactant function (38). Using PEEP also decreases extravascular lung water (74). Setting the PEEP over the lower inflection point results in an increase in the arterial oxygenation, suggesting a better gas exchange with this strategy compared with inadequate PEEP (96, 104).

The ARDS Network established the benefit of a low tidal volume ventilation strategy (105). It was found that the mortality was less in that group compared with a group ventilated with higher tidal volumes. The ventilation-free days and the days without nonpulmonary failure were more numerous than in the control group. A decrease in mortality was also observed in ventilation treatments using low tidal volumes and low inflation pressures (54) suggesting that a combined ventilation strategy consisting of low tidal volume and higher PEEP could lead to an increase in the survival rate in patients requiring mechanical ventilation (4, 38, 54). This strategy also seems to attenuate the biotrauma (54, 90). Tremblay *et al.* demonstrated that ventilation with high PEEP and a moderate tidal volume damps the increase in cytokine levels [TNFα, IL-1β,

IL-6, interferon γ (IFNγ), IL-10] in the bronchoalveolar lavage (BAL) fluid compared with ventilation strategies without PEEP in isolated rat lungs (110). The findings for the IL-6 values were confirmed for human patients by the ARDS Network (105).

In rat models of VILI, pulmonary oedema was less severe using 30 cmH_2O PIP instead of 45 cmH_2O PIP indicating a less severe process of the VILI. There is evidence that ventilation strategies for reaching a defined target end-inspiratory pressure cause milder oedema and less lung injury if these strategies include PEEP combined with a lower tidal volume (96). It has been shown that high PEEP ventilation leads to less alveolar damage by preventing alveolar instability (91). One study suggests that PEEP and low tidal volume ventilation have synergistic effects in stabilising the alveoli in which increasing PEEP has a greater effect than reducing the tidal volume (44).

There is evidence that a further improvement in survival could be achieved by additional application of recruitment maneuvers. These maneuvers may consist of a 40-second breathhold at 40 cmH_2O airway pressure (79). Other studies suggest that higher PEEP levels (above the lower inflection point) lead to a higher weaning rate from mechanical ventilation (5) and a homogenous low tidal volume ventilation (9) whereas there is no improved survival in ventilation strategies with high PEEP in comparison to lower PEEP (14).

The American-European Consensus Committee on ARDS postulated the following goals for “adequate” mechanical ventilation: 1) ensuring of an appropriate gas exchange, 2) minimising O_2 toxicity, 3) recruitment of the alveoli, 4) minimising the airway pressures, 5) prevention of atelectasis, and 6) responsible use of sedation (6).

The state-of-the-art in mechanical ventilation treatment is the ARDS Network protocol consisting of low tidal volumes, titration of respiratory rate monitored by a target pH value of 7.3 to 7.45, and a combination of inspired O_2 and PEEP leading to an oximetric saturation of 88 to 95% (40, 105). A modest hypercapnia due to low tidal volumes is permitted because it is tolerated in most patients (5, 40).

1.5. Intracellular mechanisms of converting mechanical stimuli

1.5.1. Responses to mechanical forces

Mechanical forces influence a multitude of cellular functions, including changes in cell shape, growth, differentiation, cell-cycle kinetics, apoptosis, motility, gene expression, and remodelling of the ECM (20). These mechanisms have to be seen as adaptational mechanisms to extracellular forces via intracellular signalling processes. If the mechanical stimuli are too strong, the cell membrane is destroyed. Due to this destruction the cellular adaptation becomes impossible (114).

1.5.1.1. Cell death

There are two forms of cell death. One of these is necrosis. Necrosis is a form of cell death due to cell swelling and uncontrolled disruption of the cell membrane leading to liberation of the cell contents. This, in turn, causes inflammatory responses in the direct environment of the concerned cells (47, 77). This form of cell death is thought to play a role in epithelial cell death due to alveolar overdistension (77). There is evidence that type II pneumocytes become necrotic due to increased mechanical stretch *in vitro* (46).
In contrast, apoptosis is characterised by the formation of membrane bodies, nuclear pyknosis due to condensation of the chromatin, and nuclear fragmentation. Furthermore, there is no inflammatory response in the environment of the cells because the cell contents are not liberated in a free form but in membrane bodies that can be ingested by phagocytic cells. This form of cell death is also known as controlled cell death (47).

1.5.1.2. Pro-apoptotic pathways

Apoptosis can be promoted by caspases which can be activated by released mitochondrial products as cytochrome c or the so-called death receptors. To the death receptors belong TNF receptors and the Fas receptor (77), which can be activated by TNFα or Fas ligand (47, 77). The Fas ligand exists in two forms, a soluble form and a membrane related form on the surface of cytotoxic lymphocytes (77). There are several

different targets of the caspases such as PARP [poly-adenosine diphosphate (ADP)-ribose polymerase] that are cleaved by these proteases (71). Cleavage of the targets leads to deoxyribonucleic acid (DNA) fragmentation, nuclear membrane disruption, chromatin condensation, and collapse of the cytoskeleton (71). The Fas/Fas ligand system is known to be more activated in ARDS (3, 49, 56), where the complex promotes apoptosis (3). Kitamura *et al.* demonstrated a Fas/Fas ligand-dependent mechanism of apoptosis in alveolar epithelial and endothelial cells for murine LPS-induced ALI model (56). That apoptotic mechanisms play a role in the development of ARDS is supported by the observations of Hashimoto *et al.* who found increased levels of the Fas molecule in the BAL fluid of ARDS patients (49). These findings suggest a destruction of the alveolar barrier leading to severe alveolar oedema and due to this a poor outcome of the patients. In the lung tissue of patients who died with ALI/ARDS, markers of apoptosis such as caspase-3, Bax, and p53 were found (3). *In vitro* studies demonstrated that type II pneumocytes undergo apoptosis in response to mechanical stress (46).

Another protein involved in apoptosis is p53. This protein is able to promote apoptosis in a transcription-dependent manner by recruitment of transcription factors (p53-inducible genes) and in a transcription-independent manner by cytochrome c release and caspase activation (93). One direct transcriptional target for p53 is the gene of the apoptotic peptidase activating factor 1 (Apaf1) (37). Apaf1 binds pro-caspase 9 and activates this caspase which itself activates caspase 3 (29, 64). Caspase 3, in turn, cleaves different cell proteins such as PARP or retinoblastoma proteins leading to apoptosis (64). Another target of p53 is the p21 encoding gene CDKN1A (cyclin-dependent kinase inhibitor 1a), which regulates several different cellular functions. Generally, p53 leads, via CDKN1A expression, to cell cycle arrest, not to apoptosis (7, 27, 28). Further findings underscore an anti-apoptotic role of CDKN1A, since Lu *et al.* demonstrated the induction of CDKN1A by activating the phosphoinositide 3-kinase (PI3K)/Akt pathway leading to cell protection from p53-induced apoptosis in prostate cancer (72). There is also evidence that p21 expression is dependent upon Akt phosphorylation in ovarian carcinoma cell lines and endothelial cells (82, 100). In human urothelial carcinoma cells, activation of the PI3K-Akt pathway leads, via suppression of GSK3β (glycogen synthase kinase 3β) and activation of mTOR (mammalian target of rapamycin), to CDKN1A induction (124).

A further target of p53 is the growth arrest and DNA damage gene 45a (GADD45A). GADD45A can also be induced in a p53-independent manner, which leads usually to cell cycle arrest and induction of DNA repair (7, 88). Whether Gadd45 is involved in pro- or anti-apoptotic mechanisms depends on the interaction partner recruited. In cooperation with p53, Gadd45 is pro-apoptotic (66). Gadd45a is able to act in an anti-apoptotic fashion by interaction with β-catenin or Akt (80, 111). In a pneumonia ARDS model, it was shown that Gadd45a-deficient mice sustain a higher vascular barrier dysfunction than others because of an inadequate degradation of Akt (80).

An overproduction of reactive oxygen species (ROS) is known to induce both apoptosis and necrosis (47). Reactive oxygen species can be increased in VILI due to mechanical stress (1, 19).

Mitogen-activated protein kinases play also an important role in conversion of pro-apoptotic stimuli, in particular p38 and JNK (see section 1.5.1.4). An overview of some pro-apoptotic pathways is provided in Figure 4.

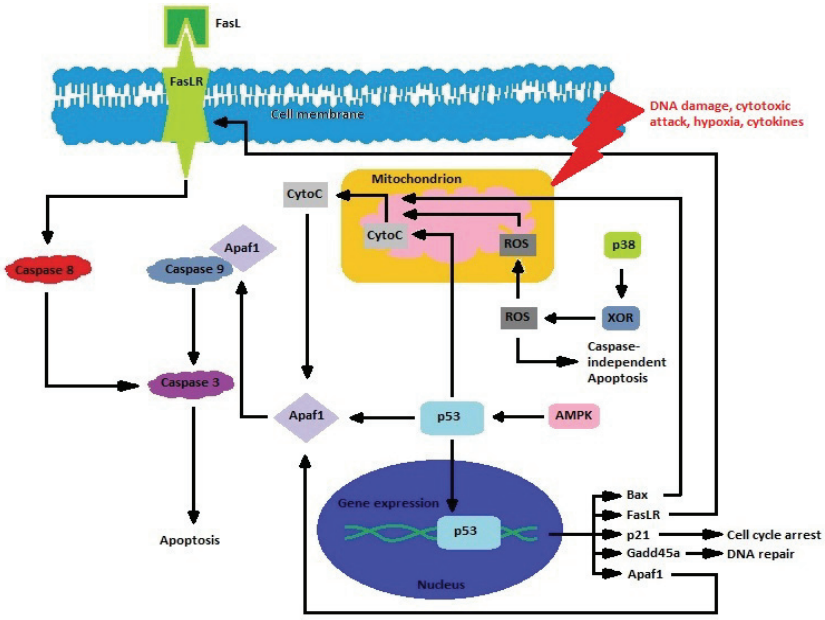

Figure 4: Overview of some pro-apoptotic mechanisms. CytoC: cytochrome c, FasL: Fas-ligand, FasLR: Fas-ligand receptor, ROS: reactive oxygen species, XOR: xanthine oxido-reductase.

1.5.1.3. Anti-apoptotic pathways

Stretch can activate phospholipase c (PLC)-γ directly, or stretch activates protein tyrosine kinases (PTK) that activate, in turn, PLC-γ. The activated PLC-γ divides phosphatidylinositol-4,5-bisphosphate (PIP2) into diacylglycerol (DAG) and inositol-1,4,5-trisphosphate (IP3). This leads to an increase of Ca^{2+} influx into the cell and activation of the protein kinase c (PKC). It is known that this pathway is involved in proliferation of foetal rat lung cells in response to cyclic stretch and strain (70, 123).

Phosphoinositide 3-kinase is also able to cleave PIP2 into DAG and IP3 (65). This kinase is activated during high PIP ventilation due to an increase in intracellular Ca^{2+} concentration by a Ca^{2+} entry through stretch activated ion channels (83). Other possibilities of PI3K activation are the activation by hepatocyte growth factor (HGF) (45, 69), keratinocyte growth factor (KGF) (8, 45), IL-1β (80), bradykinin (45) and transforming growth factor (TGF)-β (23) as well as platelet-derived growth factor (PDGF) (108). It can also be activated by ROS (2).

Phosphoinositide 3-kinase phosphorylates different downstream target proteins. One of these targets is Akt. Akt phosphorylates GSK3β that is inactivated in a phosphorylated state (69, 83, 108). Dephosphorylated GSK3β is involved in neutrophil infiltration into the lung, in apoptosis, in TNF-α and IL-1β production, and in lung injury (26). Further, active GSK3β initiates the degradation of β-catenin by phosphorylation. It is known that β-catenin plays a crucial role in the integrity of adherens junctions and for the maintenance of the blood-gas barrier in the lung. Phosphorylation of β-catenin leads to reduced epithelial and endothelial barrier properties. Taken together, Akt prevents blood-gas barrier dysfunction following the development of oedema (69, 83).

An important function of Akt is the inhibition of apoptosis (45, 83, 108). Different aspects of the anti-apoptotic effects of Akt have been discussed. Akt seems to preserve the mitochondrial membrane by preventing cytochrome c release. Further, Akt is known to inhibit pro-apoptotic proteins in a direct and an indirect manner. Finally, Akt modulates gene transcription by phosphorylation of different transcription factors, such as forkhead or nuclear factor-κB (NF-κB) (125). The Akt deactivation is associated with cell death in several cell systems. One study suggests a dependence of the activation status of Akt on nitric oxide and Ca^{2+} (76) suggesting a pro-apoptotic effect of gadolinium-sensitive Ca^{2+} channels (119) and of eNOS (endothelial nitric oxide synthase) (21) leading to vascular barrier dysfunction in response to mechanical stress

in VILI. Prevention of stretch-induced apoptosis in type II pneumocytes seems to be possible by activating the PI3K-Akt pathway (45).

There is evidence that the PI3K-Akt pathway leads to an enhanced expression of FGF2 (fibroblast growth factor 2) (17, 113, 127). Fibroblast growth factor 2 is known to play a crucial role in cell survival via the PI3K-Akt pathway due to binding the FGF receptor *inter alia* in epithelial cells (120). Thus, it is conceivable that a mechanism exists of autocrine/paracrine self-induction of FGF2 expression via Akt leading to cell survive as described for malignant carcinoma cells (12). Another factor that is influenced by Akt-mediated gene expression is HGF (113) that regulates gene expression via Akt (61). Gnecchi *et al.* postulate a paracrine upregulation of HGF (and FGF2) via Akt leading to cytoprotection in cardiomyocytes (41). An augmentation of HGF in ALI (24) is described as well as a crucial role of HGF in self-repair and anti-apoptotic mechanisms in lung cells (85).

A further function of the PI3K-Akt pathway is the regulation of cell proliferation (94). By stimulation of glucose metabolism, Akt increases intracellular ATP (adenosine triphosphate) levels. Low ATP levels are a sign of poor energy status of the cell, and can lead to controlled cell death (42). Adenosine monophosphate (AMP)-activated protein kinase (AMPK) is a kinase that acts as an energy status sensor that is activated by an increase in the intracellular AMP:ATP ratio, signalling a low energy state of the cell (48, 84). Activation of AMPK can lead to cell cycle arrest or apoptosis via p53 (48, 84, 93). Another target of AMPK is mTOR, a factor involved in protein synthesis and cell growth. AMPK is able to inhibit mTOR (48, 84). Taken together, Akt is able to inhibit AMPK activation indirectly by increased production of ATP.

Akt has also been shown to play a role in the neutrophil activation in ALI (125). Li *et al.* presented data that suggest that high tidal volume ventilation combined with hyperoxia leads, via Akt, to an augmentation of eNOS expression leading to lung neutrophil infiltration (63).

Another target of PI3K is Src, a protein that promotes β-catenin degradation. Src leads to an increase in vascular permeability. The fact that there is gross oedema in high PIP ventilated mice is explained by Miyahara *et al.* in the way that there is an imbalance between the PI3K modulated downstream effects in favour of the Src pathway (83). Mitogen-activated protein (MAP) kinases may be involved in anti-apoptotic pathways as well (see section 1.5.1.4). An overview of some anti-apoptotic pathways is provided in Figure 5.

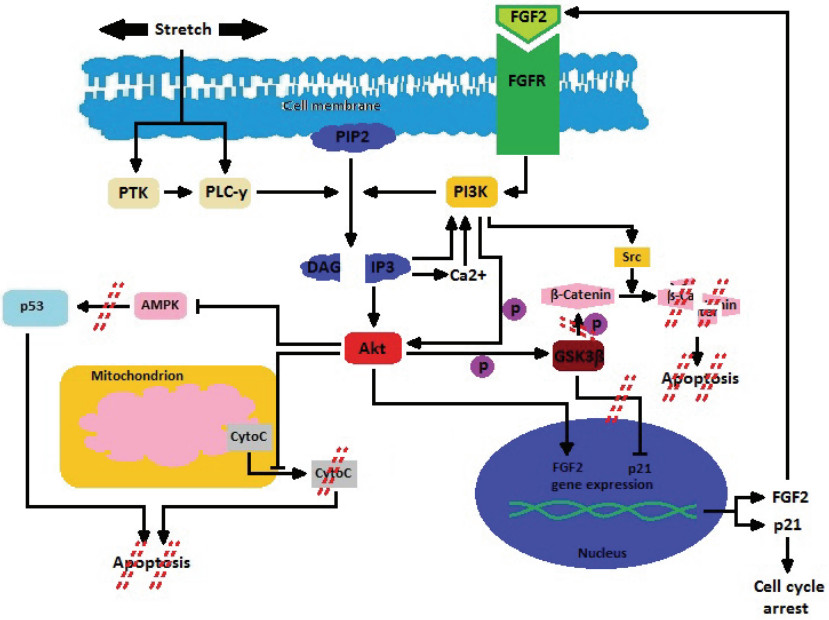

Figure 5: Overview of anti-apoptotic mechanisms via Akt. CytoC: cytochrome c, FGFR: fibroblast growth factor receptor, P: phosphate. The interrupted lines indicate the consequences of Akt activation.

1.5.1.4. Mitogen-activated protein kinase pathways

There are four known mammalian MAP kinases that are phosphorylated (and thus activated) by different MAP kinase kinases. The mitogen-activated protein/extracellular signal-related kinase kinases (MEK) 1 and 2 activate extracellular signal-related kinases (ERK) 1 and 2, the mitogen-activated protein kinase kinases (MKK) 3 and 6 activate p38, MKK4/7 activate c-Jun amino-terminal kinase (JNK), and MEK5 activates ERK5 (18, 25).

Uhlig *et al.* demonstrated that the MAP kinases JNK and ERK1/2 are more phosphorylated in rats ventilated with high pressure compared with normally ventilated rats, but saw no differences in p38 phosphorylation (115). The ERK activation due to mechanical stress was confirmed for rat pneumocytes (22). In contrast, it was also

observed activation of p38 and ERK 1 and 2 in high tidal volume ventilated mice, but no difference in the activation state of JNK was noted (1). MAP kinases are known to transduce extracellular stimuli to the nucleus where they modify gene expression (18, 115). Further, MAP kinases can modulate gene expression via post-transcriptional modification of messenger ribonucleic acid [mRNA; (18)].

The ERK activation can be explained by ligand binding to the epidermal growth factor receptor (EGFR) (112, 121). The EGFR has been shown to be up-regulated due to stretch (31). There is evidence that the EGFR is necessary for mechanotransduction in alveolar epithelial cells independent of ligand binding (22). Other mitogens that are able to activate the ERK cascade are KGF (94), PDGF, TGF-β (121) and insulin (25). Activation of these receptors leads to activation of the MAPK pathway via the G-protein Ras (25, 30, 117), whereas the mechanotransduction seems to be independent of Ras (22). Further, there is evidence that lung epithelial cells may activate ERK cascades via Fas/Fas ligand interactions *in vitro* (92). Finally, the ERKs as well as p38 and JNK can be phosphorylated in response to KGF binding to a receptor on type II pneumocytes leading to proliferation and differentiation (95). ERKs are known to be involved in cytokine production (25, 89, 92), cell proliferation (94) and prevention of apoptosis due to hyperoxia (15) as well as in activation of the xanthine oxidoreductase (XOR), an enzyme that can generate ROS, due to mechanical stress (1).

The p38 kinase is also known to play a role in the XOR activation. XOR activation is discussed to play an important role in loss of the blood-gas barrier function in VILI (1). Reactive oxygen species are increased generated in VILI leading to oxidant stress and a following increase of production of IL-1β, IL-6, and TNFα (19). The ROS are also known to play an important role in murine lung epithelial cell death due to hyperoxia (1). The kinase p38 by itself is also very important for the gene expression of TNF, IL-1, IL-6, and IL-8 (25, 89). Further, p38 can phosphorylate the GSK3β (69, 107). Finally, there is evidence that p38 may be involved in TGF-β1-induced blood-gas barrier dysfunction (13).

Ning and Wang postulate a key role for ERK1/2 and p38 in cellular response to mechanical ventilation (87). It was observed an activation of these MAP kinases via PKC leading to transcription of pro-inflammatory chemokines encoding genes due to activation of NF-κB (87). It has been shown that activation of ERK1/2 due to MEK1/2 activation may lead to an increased degradation and inactivation of the transcription-

related peroxisome proliferator-activated receptor PPARγ. Due to this inactivation the ERK1/2 may be responsible for lung injury in sepsis (55).

Extracellular signal-related kinases 1 and 2 are considered to be important for cell survival, whereas JNK and p38 may induce apoptosis via Fas ligand induction (18). A reduction of apoptosis in p38- and JNK-deficient mice under moderate tidal volume ventilation has been demonstrated, as well as a decrease in oedema levels in JNK-deficient mice, suggesting an important role for p38 and JNK in development of VILI (32). Further, there is evidence that p38 activation by TGF-β1 is involved in pro-apoptotic mechanisms in lung epithelial cells (116). Taken together, there are findings suggesting both pro-survival and cell death roles for ERK1/2. The JNK and p38 are involved in cell death mechanisms.

1.6. Aim of the study

The hypothesis of this study was that *intracellular signalling pathways in pneumocytes protect cells from damage in an "open lung" ventilation strategy compared to low PEEP and high PIP ventilated lungs*.

The goal of this study was to identify molecular mechanisms that could be involved in the protection of the lung tissue during the lung protective ventilation strategy using high PEEP and low tidal volumes in contrast to a ventilation strategy using lower PEEP in a saline washout ARDS rat model. This would be determined as follows:

1) Nucleic acids and proteins would be extracted from the lung tissues.
2) The activation of cell protective and cell death pathways would be examined.
3) Areas of cell death in ventilated lungs would be examined to identify the affected cell type.

2. MATERIALS AND METHODS

2.1. Materials

2.1.1. Equipment

Block heater HBT 130	HLC, Germany
Cannula 22G	BD, Netherlands
Centrifuge Biofuge fresco	Kendro Laboratory Products, USA
Developing machine; X Omat 2000	Kodak, USA
Falcon tubes: 15 ml, 50 ml	Greiner Bio-One, Germany
Film cassette	Sigma-Aldrich, Germany
Filter Tip FT: 10, 20, 100, 200, 1000	Greiner Bio-One, Germany
Fluorescence microscope; Leica AS MDW	Leica, Germany
Freezer -80 °C	Heraeus, Germany
Fridge +4 °C	Bosch, Germany
Fusion A153601 Reader	Packard Bioscience, Germany
Glass bottles: 250 ml, 500 ml, 1000 ml	Fischer, Germany
GS-800™ Calibrated Densitometer	Bio-Rad, USA
Hyperfilm™ ECL High Performance	Amersham Biosciences, UK
Mini spin centrifuge	Eppendorf, Germany
Microtom Micron cool-cut HM355S	Micron, Germany
Mortar	Haldenwanger, Germany
Multipette® plus	Eppendorf, Germany
Nanodrop® spectrophotometer	Peqlab, Germany
Nebuliser	Penn-Century, USA
Needle 20G	Becton Dickinson S.A., Spain
PAP pen	Sigma-Aldrich, Germany
PCR thermocycler	MJ Research, USA
Pestle	Haldenwanger, Germany
Pipetman: P10, P20, P100, P200, P1000	Gilson, France
Pipette tip: 200 µl, 1000 µl	Sarstedt, Germany
Pipette tip: 10 µl, 20 µl, 100 µl	Gilson, USA

Platform shaker Titramax 1000	Heidolph, Germany
Power supply; PowerPac 300	Bio-Rad, USA
Roto-Shake Genie	Scientific Industries, USA
Scalpel	FEATHER, Japan
Scientific Imaging Film X-OMAT™ LS	Kodak, USA
Test tubes: 0.8 ml, 1.5 ml, 2.0 ml	Greiner Bio-One, Germany
Test Tube Shaker	Merck Eurolab, Germany
Thermo-Fast® 96 PCR plate	Thermo Scientific, USA
Trans-Blot® Transfer Medium	Bio-Rad Laboratories, USA
Ventilator Servo 300	Siemens Elema, Sweden
Western blot chambers: Mini Trans-Blot	Bio-Rad, USA

2.1.2. Reagents

Acrylamide solution, Rotiphorese Gel 30	Roth, Germany
Alexa Fluor 488 goat anti-mouse IgG	Invitrogen, USA
Alexa Fluor 555 goat anti-rabbit IgG	Invitrogen, USA
Ammonium persulfate	Promega, USA
Bovine serum albumin	Sigma-Aldrich, Germany
Bromophenol blue	Sigma-Aldrich, Germany
Complete ™Protease Inhibitor	Roche, Germany
4′,6-Diamidino-2-phenyl-indol-dihydrochloride	Sigma-Aldrich, Germany
DEPC water	Roth, Germany
Dithiothreitol	Promega, USA
Dulbecco's phosphate buffered saline 10×	PAA Laboratories, Austria
ECL Plus Western Blotting Detection Reagents	Amersham Biosciences, UK
Ethylenediaminetetraacetic acid	Promega, USA
Ethylene glycol-tetraacetic acid	Sigma-Aldrich, Germany
Glycerol	Merck, Germany
β-glycerophosphate	Sigma-Aldrich, Germany
Glycine	Roth, Germany
Hydrochloric acid	Sigma-Aldrich, Germany
Isoflurane	Pharmachemie, Netherlands
β-mercaptoethanol	Sigma-Aldrich, Germany

Methanol	Fluka, Germany
N,N,N′,N′-tetramethy-ethane-1,2-diamine	Bio-Rad Laboratories, USA
Nonfat dry milk	Nestlé, Switzerland
Pancuronium bromide	NV Organon, Netherlands
Pentobarbital	Ceva Sante Animale, Netherlands
Platinum® SYBR® Green qPCR SuperMix-UDG kit	Invitrogen, USA
Precision Plus Protein™ Standards	Bio-Rad Laboratories, USA
QuickStart™ Bradford Protein Assay	Bio-Rad Laboratories, USA
RNeasy Protect Mini Kit	Qiagen, Germany
Sodium citrate	Merck, Germany
Sodium dodecyl sulfate	Promega, USA
Sodium *ortho* vanadate	Sigma-Aldrich, Germany
Sodium pyrophosphate	Sigma-Aldrich, Germany
SuperScript™III First-Strand Synthesis System	Invitrogen, USA
Super Signal® West Pico Luminol/Enhancer Solution	Pierce Biotechnology, USA
Super Signal® West Pico Stable Peroxide Solution	Pierce Biotechnology, USA
Tris	Roth, Germany
Tris-Cl	United States Biochemical, USA
Triton X-100	Promega, USA
Tween 20	Sigma-Aldrich, Germany
VECTASHIELD mounting medium	Vector Laboratories, USA

2.2. Methods

2.2.1. Animal models

All procedures were approved by the experimental animal committee of the Erasmus Medical Center (Rotterdam, Netherlands). All animals were handled in strict accordance with the European Community Guidelines. Tissue samples were obtained from specific

pathogen-free male Sprague Dawley rats of 300 g (298 - 331 g, Harlan, Horst, Netherlands).

The animals were anaesthetised after orotracheal intubation under gaseous anaesthesia (60% oxygen, 3% isoflurane), using a miniature nebuliser. A sterile polyethylene catheter was inserted into the carotid artery. Arterial blood gases and the blood pressure were monitored with this catheter. Thereafter, anaesthesia was changed into intraperitoneal pentobarbital sodium injections (60 mg/kg). Pancuronium bromide (2 mg/kg, intramuscular) was used to induce muscle relaxation. Lungs were ventilated using a Servo Ventilator 300 as described in Table 1.

Table 1: Ventilation settings of the different rat groups

	low PEEP (1-6)	high PEEP (7-12)	control (13-18)
PIP [cmH_2O]	28	30	14
PEEP [cmH_2O]	8	18	4
I:E	1:2	1:1	1:2
Frequency [min^{-1}]	30	50-60	30
Oxygen	100%	100%	100%
FiO_2	1.0	1.0	1.0

PIP: peak inspiratory pressure, PEEP: positive end-expiratory pressure, I:E: inspiration: expiration, FiO_2: fraction of inspired O_2

The rats were divided into three groups: six rats (numbers 1-6) were ventilated with a low PEEP ventilation setting after inducing lung injury, six rats (numbers 7-12) were ventilated with a high PEEP after inducing lung injury, and six rats (numbers 13-18) were ventilated without inducing lung injury as a control. For inducing lung injury, bronchoalveolar lavage with 1 ml/30 g body weight of isotonic saline solution (body temperature) was performed 6×.

For every rat PaO_2 and $PaCO_2$ was measured before and after lavage and 60 and 120 min after lavage.

After the rats were sacrificed by infusion of an overdose of pentobarbital sodium, the thorax was opened and the lungs collected under sterile conditions. Immediately, BAL fluid was obtained by rinsing the airways three times with saline. The BAL fluid was

centrifuged (300 × g for 19 min at 4 °C), and the supernatant and lung tissue were stored at -80 °C.

All these treatments of the rats were performed by a group from the Erasmus University in Rotterdam.

Preparations of the whole organs were defrosted from -80 °C. Organs were placed in a mortar where the lungs were separated from *bronchi* using disposable scalpels. Lungs were placed in centrifuge tubes such that one lung of each rat could be used for protein and RNA investigations and one lung for histology analyses.

2.2.2. Protein isolation from lungs

Frozen lung tissue was crushed into powder under liquid nitrogen with a mortar and pestle. The powder was completely covered with lysis buffer (Table 2) for extracting proteins from tissue. The pH of the Tris was adjusted with hydrochloric acid. The phosphatase inhibitor sodium vanadate and the protease inhibitor cocktail were added immediately prior to use. The lysate was passed 5-8 × through a syringe needle (20 G) to fragment larger clusters of tissue. The lysate was placed in a centrifuge tube (2.0 ml) which was placed on ice for 30 min. Every 5 min, the sample was vortexed. The lysate was centrifuged at 4 °C at 13,000 rpm for 15 min. The supernatant was aliquoted into 0.8 ml centrifuge tubes and frozen at -80 °C for further experiments.

Table 2: Composition of the lysis buffer

INGREDIENTS	CONCENTRATION
Tris (pH 7.5)	20 mM
sodium chloride	150 mM
EDTA	1 mM
EGTA	1 mM
Triton X-100	1 %
Sodium pyrophosphate	2.5 mM
β-glycerolphosphate	1 mM
sodium vanadate	10 µl/ml
Complete™ Protease Inhibitor	40 µl/ml

EDTA: ethylenediaminetetraacetic acid, EGTA: ethylene glycol tetraacetic acid

2.2.3. Determination of protein concentration

After thawing, the protein concentration in the lysate was determined colometrically using a Bradford Protein Assay. Quick Start™ Bradford Dye Reagent (200 µl) was mixed with 20 µl of a 1:100 protein dilution. After an incubation of 15 min at room temperature the absorbance was measured at a wavelength of 570 nm with the Packard Fusion™ instrument. The protein concentration was calculated using the standard curve using Microsoft Excel.

2.2.4. SDS polyacrylamide gel electrophoresis

Proteins were separated using sodium dodecyl sulfate polyacrylamide gel electrophoresis (SDS-PAGE). The SDS denatures proteins, binds to the polypeptides, and provides a consistent negative charge to the polypeptides allowing a migration of the proteins to the positive electrode in an electric field. The mobility of the proteins correlates negative with the protein size: larger proteins migrate slower than smaller ones. According to the molecular weight, the proteins can be separated.
With 2× SDS loading buffer (Table 3) were combined 150 µg of protein. This mixture was heated at 95 °C for 10 min in a water bath before it was loaded onto the gel consisting of resolving gel (Table 4) and stacking gel (Table 5). Electrophoresis was carried out in running buffer (Table 6) at 90 V until the front dye reached the bottom of the gel.

Table 3: Composition of the loading buffer

INGREDIENTS	CONCENTRATION
Tris, pH 6.8	100 mM
SDS	4%
Bromophenol blue	0.2%
Glycerol	20%
DTT	200 mM

SDS: sodium dodecyl sulfate, DTT: dithiothreitol

Table 4: Composition of the resolving gel

INGREDIENTS	AMOUNT FOR 1 GEL
Distilled water	4 ml
30% acrylamide	3.3 ml
1.5 M Tris, pH 8.8	2.5 ml
10% SDS solution	100 µl
10% APS	100 µl
TEMED	4 µl

SDS: sodium dodecyl sulfate, APS: ammonium persulfate, TEMED: N,N,N′,N′-tetramethy-ethane-1,2-diamine

Table 5: Composition of the stacking gel

INGREDIENTS	AMOUNT FOR 1 GEL
Distilled water	3.4 ml
30% acrylamide	0.8 ml
1,0 M Tris, pH 6.8	0.6 ml
10% SDS solution	50 µl
10% APS	50 µl
TEMED	5 µl

SDS: sodium dodecyl sulfate, APS: ammonium persulfate, TEMED: N,N,N′,N′-tetramethy-ethane-1,2-diamine

Table 6: Composition of 10× running buffer

INGREDIENTS	AMOUNT per 1 l
Tris	30 g
Glycine	144 g
10% SDS solution	100 ml

SDS: sodium dodecyl sulfate

2.2.5. Protein blotting

A western blot allows detection of specific proteins in protein mixtures using specific antibodies for recognition. For antibody interaction the proteins have to be transferred from the polyacrylamide gel to a 0.25 nitrocellulose membrane. For protein transfer was used an electric field of 90 V for a duration of 90 min. The procedure was performed in blotting buffer (Table 7).

Table 7: Composition of the blotting buffer

INGREDIENTS	CONCENTRATION
Methanol	20%
Tris	20 mM
Glycine	150 mM

The membranes were then washed 2×5 min while shaking on a Roto-Shake Genie (Table 8).

Table 8: Composition of the washing buffer

INGREDIENTS	AMOUNT
10× Dulbecco's PBS	100 ml
Tween 20	1 ml
Distilled water	filled up to 1 l

PBS: phosphate buffered saline, PBST: PBS/Tween 20

2.2.6. Protein visualisation

At room temperature, membranes were blocked while shaking in blocking buffer for 1 h (Table 9) followed by incubation with the appropriate primary antibodies during shaking on a platform shaker at 4 °C overnight. The membranes were washed 3×10 min with washing buffer and then incubated with a horse-radish peroxidase (HRPO)-linked secondary antibody for 2 h at room temperature followed by 3×10 min washing. The concentrations of the primary and secondary antibodies are presented in Table 10.

Specific bands were detected by using the Super Signal® West Pico Luminol/Enhancer Solution and the Super Signal® West Pico Stable Peroxide Solution. When the signal was too weak or not detectable, the ECL Plus Western Blotting Detection Reagents A and B were used.

Table 9: Composition of the blocking buffer

INGREDIENTS	CONCENTRATIONS
PBST	Table 8
Nonfat dry milk	5 %

PBST: phosphate buffered saline/Tween 20

Table 10: Primary antibodies used in this study

ANTIBODY	DILUTION	DILUTED IN	SOURCE	DILUTION Secondary antibody	CATALOGUE #	COMPANY
Phospho-Akt	1:1000	BSA	rabbit	1:2000	9271	Cell Signaling
Akt	1:1000	BSA	rabbit	1:5000	9272	Cell Signaling
Phospho-AMPKα	1:667	BSA	rabbit	1:2000	2535	Cell Signaling
AMPKα	1:1000	BSA	rabbit	1:2000	2532	Cell Signaling
Phospho-β-Catenin	1:500	BSA	rabbit	1:1000	9561	Cell Signaling
β-Catenin	1:1000	BSA	rabbit	1:2000	9562	Cell Signaling
Phospho-GSK3β	1:1000	BSA	rabbit	1:2000	9336	Cell Signaling
GSK3β	1:2000	BSA	rabbit	1:2000	9315	Cell Signaling
MEK1/2	1:1000	BSA	rabbit	1:5000	9122	Cell Signaling
Phospho-p38	1:500	BSA	rabbit	1:5000	9211	Cell Signaling
p38	1:1000	BSA	rabbit	1:5000	9212	Cell Signaling
Phospho-p44/42	1:500	Milk*	mouse	1:1000	9106	Cell Signaling
p44/42	1:1000	BSA	rabbit	1:5000	9102	Cell Signaling
p53	1:2000	BSA	rabbit	1:2000	2527	Cell Signaling
Cleaved PARP	1:1000	Milk*	rabbit	1:2000	9545	Cell Signaling
PARP	1:1000	Milk*	rabbit	1:2000	9542	Cell Signaling
Phospho-SAPK/JNK	1:500	BSA	rabbit	1:1000	9251	Cell Signaling
SAPK/JNK	1:1000	BSA	rabbit	1:4000	9252	Cell Signaling

***Milk = blocking buffer; BSA: bovine serum albumin, AMPKα: adenosine monophosphate-activated protein kinase α, GSK3β: glycogen synthase kinase 3β, MEK1/2: mitogen-activated protein/extracellular signal-related kinase kinases 1/2, PARP: poly-ADP-ribose polymerase, SAPK: stress-activated protein kinase, JNK: c-Jun-NH2-terminal kinase.**

The luminescence of the HRPO product was detected with Kodak Scientific Imaging Film or the more sensitive Hyperfilm™ ECL High Performance chemiluminescence film.

The membranes were rinsed with washing buffer (1×10 min) before stripping in a water bath of 60 °C for 10 min. For this procedure the membranes were put into a Falcon tube with stripping buffer (Table 11). This procedure allows detection of the phosphorylated form and thereafter of the total amount of the appropriate protein with one membrane, using the described instructions.

Table 11: Composition of 100 ml of stripping buffer

INGREDIENTS	VOLUME
Double-distilled water	91.7 ml
10% SDS solution	2 ml
1.0 M Tris pH 6.8	6.25 ml
β-mercaptoethanol	0.7 ml

SDS: sodium dodecyl sulfate

2.2.7. RNA isolation

Isolation of RNA from lung tissue was performed according to the manufacturer's instructions provided with RNeasy Protect Mini Kit containing amongst others the buffers RLT, RW1, and RPE.

The RNA isolation and RNA handling until cDNA synthesis were performed under cold conditions to prevent RNA degradation. For cooling tissue and/or the centrifuge and collection tubes was used liquid nitrogen.

A lysis buffer containing 20 µl of 2 M DTT per 1 ml RLT buffer was prepared before RNA isolation. Analogous to the protein isolation, frozen lung tissue was crushed into powder under liquid nitrogen with a mortar and pestle. The lysis buffer (600 µl) was added before a 2 min centrifugation in a cooled 2 ml centrifuge tube followed. Accordant with the homogenisation of the tissue for the protein analysis, the homogenisation was performed with a needle and syringe. The lysate was centrifuged for 3 min before the supernatant was transferred to a new centrifuge tube. At the rate of

1:1 ethanol (70%) was added. This was mixed by pipetting. The mixture was transferred into a combination of RNeasy spin column and collection tube before 15 sec of centrifugation (8000 × g). The flow-through was discarded. With 700 µl of RW1 buffer it was performed an anew centrifugation for 15 sec at 8000 × g. After discarding the flow-through the RNeasy spin column was washed two times with 500 µl of buffer RPE. This was performed by one 15 sec and one 2 min centrifugation at 8000 × g. Adding 50 µl of RNA free water followed by 1 min centrifugation at 8000 × g led to elution of the RNA.

2.2.8. Measuring RNA concentration

The concentration and quality of the obtained RNA was determined by measuring the optical density of the obtained solutions with a Nanodrop® spectrophotometer. The leachate (10 µl) was mixed with 490 µl of 7.0 pH Tris-Cl. The absorbance of the diluted sample was measured at 260 nm. The amount of RNA was calculated by using the formula $C=A_{260} \times 44$ µg/ml × 50 where C is the concentration, A_{260} is the measured absorbance, 44 µg/ml is an absolute term describing the correlation of absorbance to the concentration of RNA (1 unit absorbance corresponds to 44 µg RNA per ml), and 50 is the dilution factor. By multiplication with the volume of the elution the total amount of RNA was calculated.

2.2.9. cDNA synthesis

Reverse transcriptase is a RNA-dependent DNA polymerase that transcribes the mRNA of the obtained solutions into complementary DNA (cDNA). Total RNA (5 µg) was combined with 1 µl of random hexamers, 1 µl of dNTP mix and autoclaved water up to 10 µl total volume. The mixture was incubated at 65 °C for 5 min, chilled on ice for 1 min, and 10 µl of cDNA Synthesis Mix (Table 12) was added. After gentle mix and brief centrifugation these mixtures were incubated at 25 °C for 10 min followed by an incubation of 50 min at 50 °C. With a temperature increase to 85 °C for 5 min the reactions were stopped by inactivating the reverse transcriptase. The mixtures were put

on ice immediately before 1 µl of *E. coli* RNase H was added. The cDNA was generated after a further incubation at 37 °C for 20 min.

Table 12: cDNA Synthesis Mix

REAGENTS	VOLUME
10× RT buffer	2 µl
25 mM $MgCl_2$	4 µl
0.1 M DTT	2 µl
RNaseOUT™	1 µl
SuperScript™ III RT	1 µl

RT: reverse transcriptase, DTT: dithiothreitol

2.2.10. Real-time polymerase chain reaction

Quantitative real-time PCR (qPCR) is used to amplify and quantify a specific DNA molecule, where SYBR Green I can be used as a detection system, as SYBR Green I is a double-stranded DNA intercalating dye that fluoresces once bound to double-stranded DNA. The amount of bound dye correlates with the amount of target amplicon generated.

The reactions were performed according with the manufacturer's instructions provided the Platinum® SYBR® Green qPCR SuperMix-UDG kit (Table 13).

Table 13: Composition of the real-time polymerase chain reaction

REAGENTS	VOLUME
Platinum® SYBR® Green qPCR SuperMix-UDG	13 µl
50 mM $MgCl_2$	1 µl
10 µM forward primer	0.5 µl
10 µM reverse primer	0.5 µl
cDNA template	2 µl
autoclaved water	8 µl

UDG: uracil-DNA glycosylase

The polymerase chain reaction was run with following settings: 2 min with 50 °C for UDG incubation, 2 min with 95 °C for the denaturation followed by 40 cycles of 15 s with 95 °C for denaturation of the double stranded DNA and 30 s with 60 °C for primer annealing and production of complementary DNA strands. The fluorescence intensity was measured at the end of the elongation phase. Hypoxanthine phosphoribosyltransferase (HPRT) is a so-called housekeeping gene - ubiquitously and constitutively-activate gene in mammals - and was used as internal control. For the comparability between the measurements it was used the $\Delta\Delta C_t$ method ($\Delta\Delta C_t = \Delta C_t(\text{treated}) - \Delta C_t(\text{control})$). The primers employed are listed in Table 14.

Table 14: Primer sequences

Gene	Accesion		Sequences (5′ → 3′)	Length	Applicon
APAF1	NM_023979	for	CGGTCACACGAACTCAGTCA	20 bp	348 bp
		rev	ACTGCCAAATGGTCGTAGGG	20 bp	
CDKN1A	NM_080782	for	AGTAGGACTTCGGGGTCTCC	20 bp	121 bp
		rev	AATGTCAAGGCTCTGGACGG	20 bp	
GADD45A	NM_024127	for	CCGCAGAGCAGAAGATCGAA	20 bp	89 bp
		rev	AGTTATGGTGCGCTGACTCC	20 bp	
RBBP7	NM_031816	for	GCTTGATTTGTCAAGCGCCA	20 bp	115 bp
		rev	ACAGTACGCAACAGCTCACT	20 bp	
RGD1561176	NM_001029910	for	AGGCTCCGTGTACTGTGTTG	20 bp	320 bp
		rev	CCTGGCACTGTACGGCTAAA	20 bp	

for: forward primer, rev: reverse primer, bp: base pairs

To exclude DNA contamination there was performed a control experiment of the PCR without reverse polymerase. If there was DNA detected the sample was contaminated. Contaminated samples were discarded.

2.2.11. Cryosections - immunohistochemistry

Immunohistochemistry is a method to detect and localise antigens in tissue sections. It is based on antibody-antigen interaction and on fluorescence, using a primary antibody

against the target antigen. A secondary antibody against the primary antibody is labelled with a fluorescent dye that can be examined by microscopy.

Lung tissue was sectioned with a cryostat. The 6 µm-thick sections were placed on a silanised slide. These slides were washed in PBS for 5 min. To make the sections permeable sections were put in permeabilisation buffer for 10 min at 4 °C. The permeabilisation buffer was produced by mixing 0.1% Triton X-100 and 0.1% sodium citrate in PBS. After permeabilisation the slices were washed out with PBS 3×5 min. For creating a hydrophobic cycle around the tissue it was used a PAP pen. The slides were incubated in 100 µl 10% BSA/PBS for 1 h at 4 °C. After this incubation the slides were washed out with PBS 3×5 min. The primary antibodies (Table 15) were diluted in 100 µl of 0.1% BSA/PBS.

Table 15: Primary antibodies used for immunohistochemistry

ANTIBODY	DILUTION	SOURCE	CATALOGUE #	COMPANY
Aquaporin 5	1:1000	rabbit	78486	Abcam, UK
SP-C	1:1000	rabbit	AB3786	Chemicon, USA
p53	1:200	mouse	2524	Cell Signaling, USA

SP-C: surfactant protein C

Incubation with the primary antibodies was performed for 1 h at 4 °C. Protein accumulation of p53 was used for the detection of apoptosis, aquaporin 5 was used as a marker for type I pneumocytes, and SP-C (surfactant protein C) as a marker for type II pneumocytes. After this incubation time, slides were washed with PBS 3×5 min before the incubation with the secondary antibodies. Secondary antibodies were Alexa Fluor 555 goat anti-rabbit IgG and Alexa Fluor 488 goat anti-mouse IgG. The incubation of the secondary antibodies was performed in the dark at 4 °C for 1 h at a dilution of 1:1000 in 100 µl 0.1% BSA/PBS. Sections were washed 3×5 min in PBS. The nuclei of all cells were labelled using DAPI (4',6-diamidino-2-phenyl-indol) that binds to DNA and fluoresces blue. At room temperature, the sections were incubated with 100 µl of 1:100 DAPI/PBS for 7 min in the dark. Then, the sections were washed 3×5 min with PBS. After incubation with secondary antibody, respectively with the DAPI the sections were covered with VECTASHIELD mounting medium for preserving the fluorescence

for the microscopic examination. Images of the save field were taken using three different fluorescence channels, to identify nuclei (DAPI), cell types (type I pneumocytes [aquaporin 5] and type II pneumocytes [SP-C]), and apoptosis (p53).

2.2.12. Statistical analysis

The qRT-PCR results were presented as means ± standard error of mean. The ΔΔCt values obtained from qRT-PCR were analysed in groups with Grubbs test to determine and exclude statistical outliers. Statistical outliers are referred in the concerning section. The data were then subjected to a two-tailed, one-sample Student's t-test for comparing two groups with each other (high PEEP vs. low PEEP, high PEEP vs. control, and low PEEP vs. control). Results were considered statistically significant when $p < 0.05$. For the statistical calculations was used GraphPad Prism 5 (GraphPad Software, USA).

3. RESULTS

3.1. Protein expression analysis

3.1.1. The mitogen-activated protein kinases

It is known that different extracellular stimuli like stretch at the cell surface evoke a change in the activation state of different MAP kinases. Figure 6 illustrates the activation states of different MAP kinases due to the different ventilation strategies, and in absence and presence of lung injury.

There was no evidence for a different abundance of phosphorylated MEK1/2 in the different treated rat groups. But the phosphorylation state of the ERK1 and ERK2 in injured rat lungs was increased compared to the lungs of non-injured rat lungs independent of the used ventilation strategy. Further, there was no difference in the abundance of phosphorylated JNK in the three different rat groups. It was noted an increase in p38 phosphorylation in lung-injured rats independent of the chosen ventilation setting.

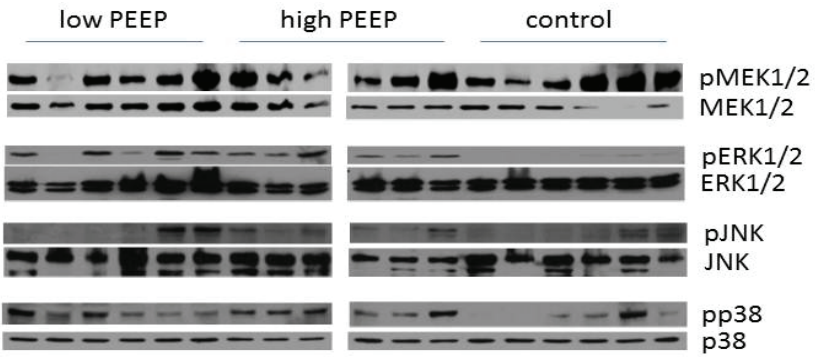

Figure 6: Phosphorylated (p) MAP kinases and total MAP kinases in the lung tissue lysates.

3.1.2. PI3K-Akt pathway

The PI3K-Akt pathway is known to be involved in cellular responses due to mechanical ventilation. Figure 7 illustrates that the fraction of phosphorylated Akt was highest in

the rat group with underlying lung injury and ventilated with high PEEP whereas the levels of total Akt were similar. The phosphorylation state of GSK3β was increased in that group. The fraction of phosphorylated β-catenin was lower in the rat group with lung injury that was ventilated with high PEEP. Furthermore, the phosphorylation state of AMPKα was lower in the group with lung injury ventilated with high PEEP. These results suggest a lung protective effect of high PEEP ventilation settings because the PI3K-Akt pathway is known to be involved in anti-apoptotic mechanisms as described in section 1.5.1.3.

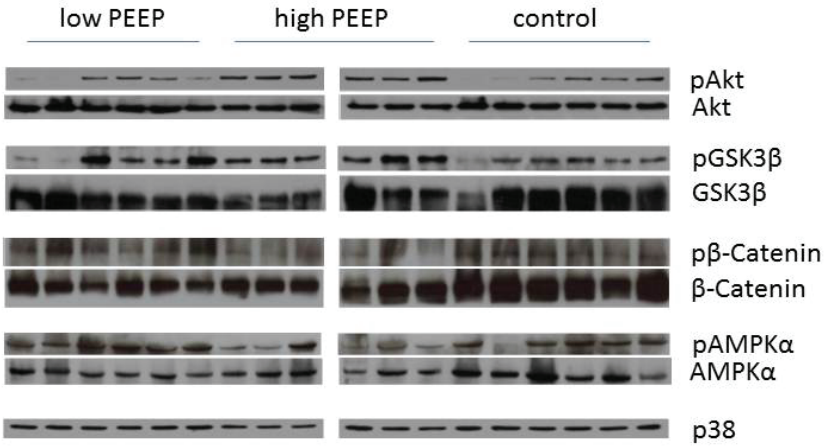

Figure 7: Expression at phosphorylation status (p) of PI3K-Akt pathway proteins in the different lung tissue lysates.

3.1.3. Markers of cell death

Both p53 and PARP were investigated as markers of cell death. Figure 8 illustrates that highest degree of cell death occured in the group of rats that was ventilated with low PEEP after inducing lung injury. The levels of the cell death markers in the rat group that was ventilated with high PEEP after lung injury were similar to the levels in that group without lung injury suggesting lung protective effects of high PEEP ventilation settings.

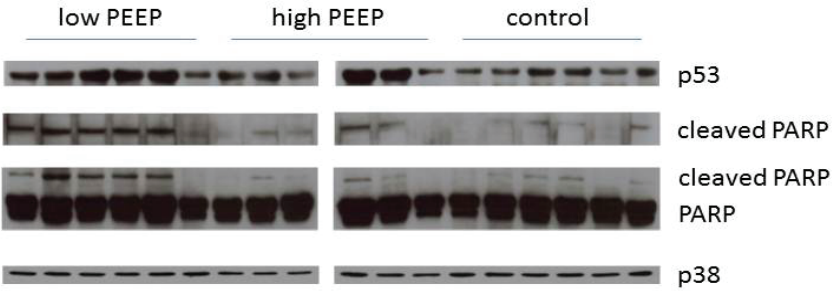

Figure 8: Cell death markers due to the different treatments of the rats.

3.2. Gene expression analysis

The amount of specific mRNA correlates with the activation state of the associated gene. Selected p53-inducible genes with known pro-apoptotic gene products were investigated in this study: Apaf1, CDKN1a and Gadd45a, as well as the pro-apoptotic but p53-independent genes retinoblastoma binding protein Rbbp7 and the rat equivalent of the ALG2 interacting protein ALIX - RGD1561176.

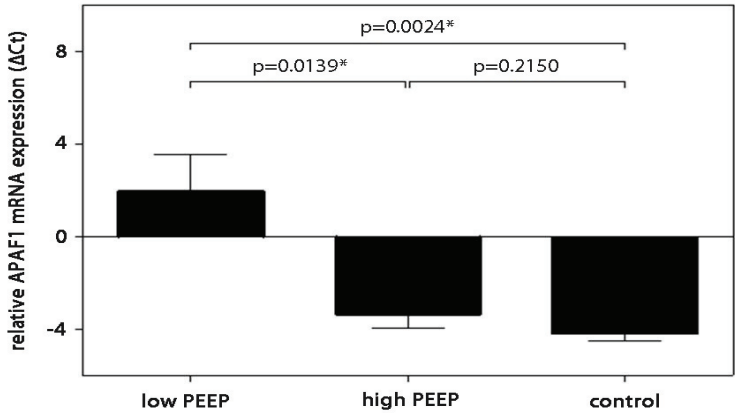

Figure 9: The gene expression of APAF1 in the low PEEP ventilated rat group, the open lung approach ventilated group and the rat group without lung injury compared with HPRT. * indicates statistical significance (p<0.05).

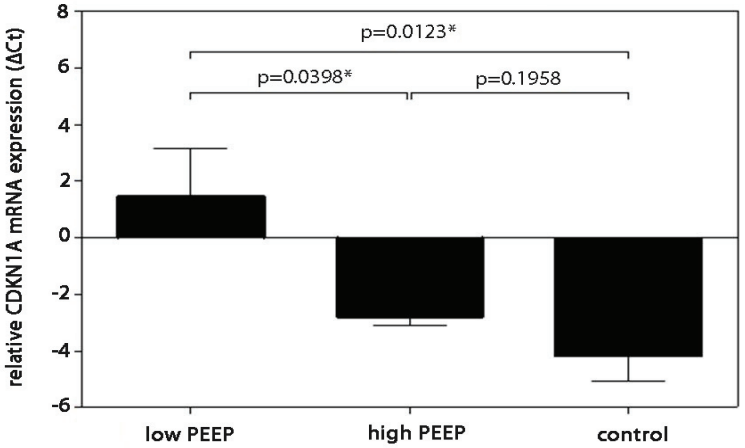

Figure 10: The gene expression of CDKN1A in the low PEEP ventilated rat group, the open lung approach ventilated group and the rat group without lung injury compared with HPRT. * indicates statistical significance (p<0.05).

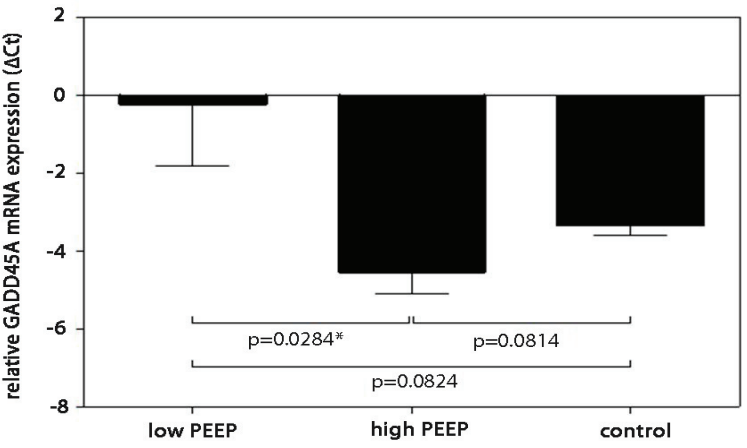

Figure 11: The gene expression of GADD45A in the low PEEP ventilated rat group, the open lung approach ventilated group and the rat group without lung injury compared with HPRT. * indicates statistical significance (p<0.05).

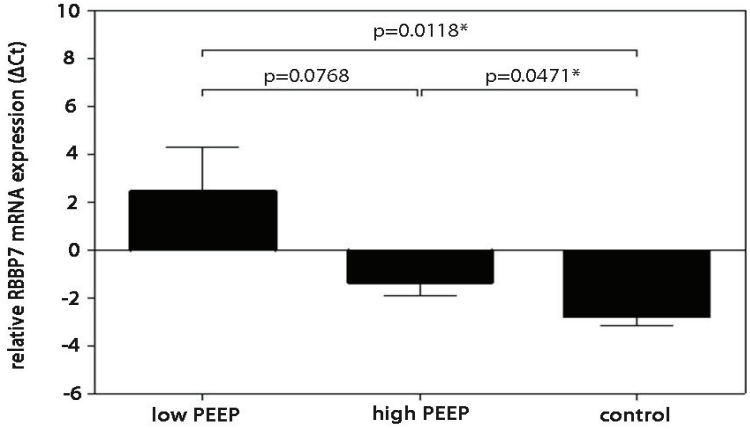

Figure 12: The gene expression of RBBP7 in the low PEEP ventilated rat group, the open lung approach ventilated group and the rat group without lung injury compared with HPRT* indicates statistical significance (p<0.05).

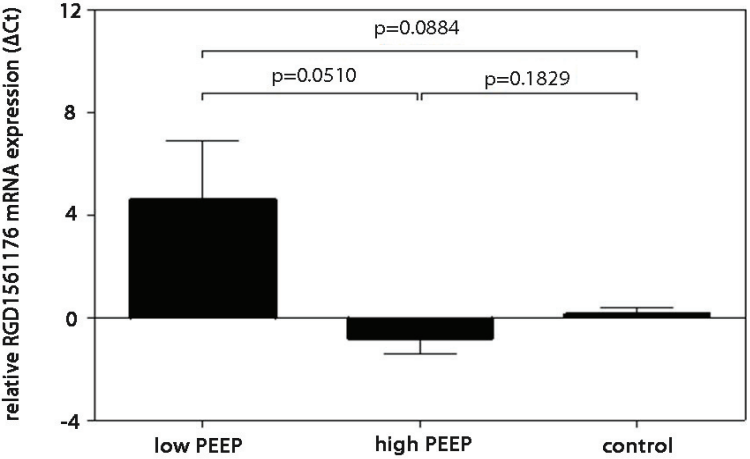

Figure 13: The gene expression of RGD1561176 in the low PEEP ventilated rat group, the open lung approach ventilated group and the rat group without lung injury compared with HPRT.

With the Grubbs test were identified as statistical outliers the values of rat 10 for the CDKN1a and the GADD45a analyses, and the value of rat 9 for the RGD1561176 analysis; these samples were excluded before the statistical calculations were done. The expression of the investigated genes was highest in the tissue lysates of the rat group that was ventilated with low PEEP ventilation approach suggesting a pro-apoptotic effect of low PEEP ventilation. Whereas the differences between the low and high PEEP ventilated rat groups were not statistically significant for the pro-apoptotic but p53-independent genes RBBP7 (Figure 12) and RGD1561176 (Figure 13), there was a statistical significance between these groups considering the expression state of the pro-apoptotic and p53-inducible genes APAF1 (Figure 9), CDKN1a (Figure 10) and GADD45a (Figure 11). Furthermore, there were no statistical significant differences in apoptotic gene expression between the high PEEP ventilated group and the control group. These findings provide an evidence of p53-dependent pro-apoptotic mechanisms in low PEEP ventilation settings whereas high PEEP ventilation seems to protect the lung leading to an outcome as if there was no lung injury. These findings corroborate the results of the protein investigations that also demonstrated a higher rate of apoptosis in the low PEEP ventilated lung tissue compared to the high PEEP ventilated group.

3.3. Immunohistochemistry

Immunohistochemistry was performed to detect the structures of the lungs that are affected the most by cell death in VILI.

Figure 14 illustrates the results with the type I pneumocyte cell marker aquaporin 5. The colocalisation of the apoptosis marker p53 with the type I pneumocyte marker suggested apoptosis in type I pneumocytes in low PEEP ventilated rats.

In Figure 15, staining for the type II pneumocyte marker SP-C is illustrated. The staining of the apoptosis marker p53 generally did not colocalise with the SP-C staining, suggesting, by comparison with Figure 14, that the p53 accumulation is largely found in type I pneumocytes rather than in type II pneumocytes. These findings permit the conclusion that the type I pneumocytes are affected more by cell death than the type II pneumocytes in low PEEP ventilated rats.

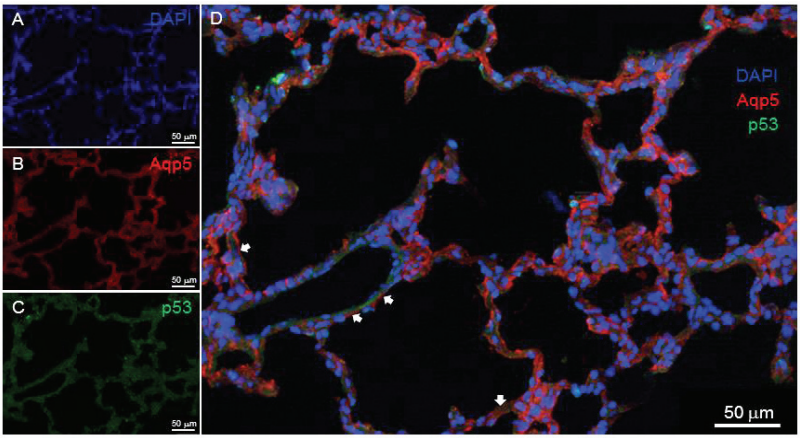

Figure 14: Images from sections from rat 1. (A) Staining with DAPI, (B) staining with aquaporin 5, (C) staining with p53 antibodies. (D) composite of the three images (A), (B) and (C). The arrows indicate the colocalisation of aquaporin 5 and p53 staining.

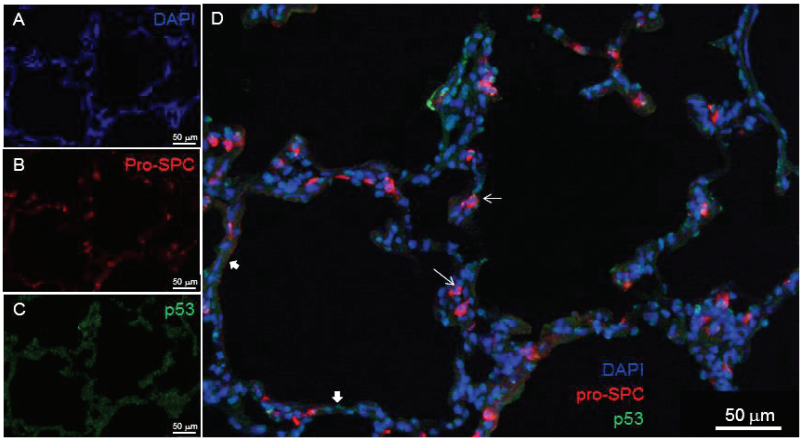

Figure 15: Images from sections from rat 1. (A) Staining with DAPI, (B) staining with S-PC, (C) staining with p53 antibodies. (D) composite of the three images (A), (B) and (C). The arrows indicate the divergence of p53 and SP-C staining (bulky arrows: p53 signal without SP-C signal, thin arrows: SP-C signal without p53 signal).

4. DISCUSSION

Acute respiratory distress syndrome is the major reason for morbidity and mortality in patients treated in intensive care units, although lung protective ventilation strategies - i.e. high PEEP ventilation strategies - lead to a decrease in mortality rate due to ARDS (68, 98, 126). The basis of ARDS is a direct or an indirect pulmonary injury (50). Mechanical ventilation is the basis of treatment of patients with ARDS (103). But mechanical ventilation may itself lead to further damage of the lung tissue by mechanical forces (34, 43, 54, 102, 118). To minimize the risk of VILI lung protective ventilatory strategies consisting of a PIP of 40-60 cmH_2O, a ratio of the duration of inspiration to expiration (I:E) of 1:1 to 2:1, a PEEP of 10-20 cmH_2O, a permissive hypercapnia, and inspiration of low levels of O_2 were developed (90).

The aim of this study was to investigate molecular pathways that could be involved in the protection of the lung tissue during the lung protective ventilation strategy using high PEEP and low tidal volumes, in contrast to a ventilation strategy using lower PEEP in a saline washout ARDS rat model.

For most investigations reported here, the whole lung tissue, not individual cells or cell types were investigated. The advantage of this kind of investigation is that the organ was treated in a natural manner because the organ was located *in situ* in the organism. All interacting mechanisms - direct lung reactions as well as systemic retroactions on the lung due to mechanical ventilation - were involved. The handicap of this method is that it was not possible to assign the observed reactions to specific cells or cell types. The immunohistochemical investigations attempted to fill this gap.

According to the pressure-volume curve illustrated in Figure 2 ventilation settings must be adapted to the pressure-volume curve as pictured in Figure 16 to prevent VILI by volutrauma or atelectrauma.
As described in the introduction, volutrauma and atelectrauma are the most important determinants of VILI (54). Volutrauma is evoked by application of high end-inspiratory volumes (43). Atelectrauma is induced by cyclic opening and collapse of the alveoli

(16, 67). In the “open lung” ventilation strategy both of them are prevented because the pressure-volume curve is approximated to the scheme in Figure 16.

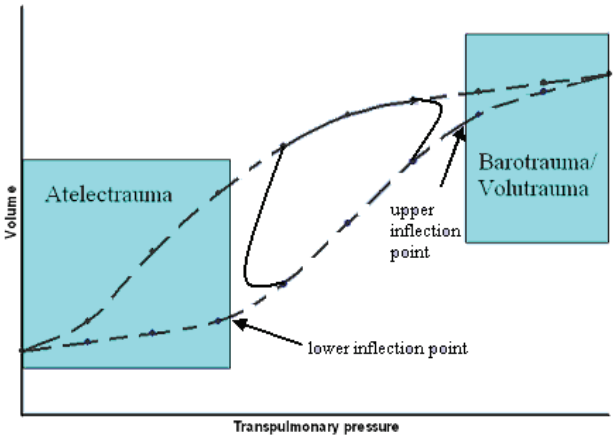

Figure 16: Approximation to the pressure-volume curve without induction of traumata leading to VILI. 2. Modified from: (102).

Barotrauma seems to be largely unimportant for the development of VILI (54, 102). The result of using this kind of ventilation strategy should be lung protective ventilation.

The MAP kinases can be activated by mitogens such as TGF-β and bone morphogenetic proteins, or due to mechanical stimuli. Two of these MAP kinases are MEK1 and MEK2. These kinases are known to be activated due to TGF-β binding to the epidermal growth factor receptor (121). Phosphorylation of MEK1/2 usually leads to ERK1/2 activation. Western blot results revealed an equal phosphorylation state of MEK1/2 in all rat groups independent of induction of lung injury and independent of the ventilation strategy (Figure 6). Whereas, with western blots it was demonstrated that the phosphorylation state of the ERKs was higher in the rat lungs with induced lung injury, but there was no difference between the two ventilation strategies (Figure 6). It is known that ERK1/2 can be activated via EGF receptors due to mechanical stimuli, such as postulated for VILI (22, 31). There are also findings that suggest a cell damaging

effect of MEK1/2-mediated ERK1/2 activation (55, 101). The western blot analyses do not allow a conclusion as to the cell origin.

Although the MEK1/2 activation state did not reveal a difference in the rat groups, the ERK phosphorylation state was equal in the lung injured rat groups but independent of the ventilation strategy increased to the non-injured rat group suggesting an upregulation due to lung injury. It can be speculated that an unknown interacting factor that is upregulated due to lung protective ventilation inhibits the ERK activation by MEK. Taken together, this would speak for a preponderance of the pro-apoptotic power of ERK in the whole lung despite possible protective effects in particular lung cells.

Another MAP kinase that is known to be activated due to pressure applied in mechanical ventilation is JNK (115). In the western blot studies, there was no difference in the phosphorylation state of the JNK comparing the absence and presence of lung injury or with different ventilation settings (Figure 6). Uhlig *et al.* compared two ventilation settings in the absence of lung injury (115). Comparable to the findings in this study, there was no significant difference in the JNK phosphorylation state. Furthermore, Abdulnour *et al.* could not find any differences in phosphorylation of JNK comparing a high tidal and a low tidal volume ventilation at all (1). Thus, it seems that differences in PEEP settings do not lead to an activation of the JNK as well as the absence or presence of ARDS.

The third MAP kinase investigated was p38, which is known to be activated by mechanical stress (1, 115). In the investigations of Uhlig *et al.* no differences were found in phosphorylation of p38 between high and low PIP ventilation (115). These findings are comparable with the results of the western blots in this study that did not reveal any differences between high and low PEEP ventilation, suggesting that the type of ventilation strategy is not relevant for p38 activation. But in the data presented here, there was a difference in phosphorylation state comparing injured and uninjured rat lungs (Figure 6). The kinase p38 is known to be an important factor in development of cell damage and blood-gas barrier dysfunction in VILI (13, 18, 32, 116).

The MAP kinase western blots suggest an activation of ERK1/2 and an activation of p38 in the saline lavaged rat lungs compared with non-injured rat lungs.

Akt is a kinase that can lead, via different steps, to inhibition of apoptosis (45, 83, 108). The Akt can prevent VILI due to PI3K activation (83). During high PIP ventilation was seen an increase of PI3K activation state (83).

Western blot analyses in this study revealed an increased Akt activation state in lung tissues of the "open lung" ventilated rats. The phospho-Akt levels in the tissues of rats that were not injured were similar to the tissue of the low PEEP ventilated rats. Consistent with these findings further western blots demonstrated increased phosphorylation states of GSK3β in the "lung protective" ventilated rat lung tissues (Figure 7). Glycogen synthase kinase 3β is a target of Akt. It is known that dephosphorylated GSK3β is involved in apoptosis and lung injury (26). Glycogen synthase kinase 3β in dephosphorylated state phosphorylates β-catenin. By phosphorylation β-catenin is marked for decomposition leading to decreased blood-gas barrier function (69, 83). The western blot analyses of β-catenin revealed that the tissue of the high PEEP ventilated rat group contained a lower level of phospho-β-catenin than the tissue of the other groups (Figure 7). Indirectly, Akt is able to inactivate another pro-apoptotic protein – the AMPKα (42, 48, 84, 93). The western blot analyses of AMPKα revealed a lower level of the AMPKα phosphorylation state in the rat group with lung injury and high PEEP ventilation compared with the other groups (Figure 7).
Figure 17 gives an overview of the found anti-apoptotic mechanisms due to the "open lung" ventilation strategy.

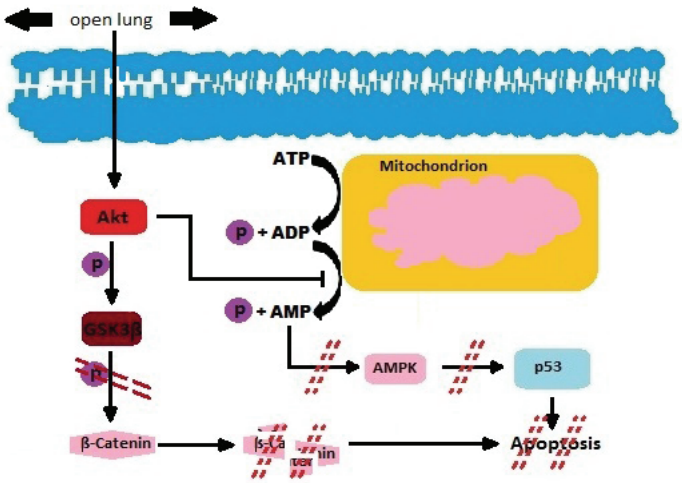

Figure 17: Summary of the lung protective cellular mechanisms via Akt in the "open lung" ventilation strategy. ATP: adenosine triphosphate, ADP: adenosine diphosphate, AMP: adenosine monophosphate, P: phosphate. The interrupted lines indicate the consequences of Akt activation.

Via p53, AMPKα is able to induce apoptosis (48, 84, 93). Further western blot analyses demonstrated that the p53 levels in the lung tissue of rats ventilated with the protective strategy were similar to the p53 levels in the tissue of the non-injured rats. In contrast, the p53 levels in the lung tissue of the low PEEP ventilated rats were higher than in the high PEEP ventilated rats and in the non-injured rats (Figure 8). Another marker of cell death is cleaved PARP (71). Western blots revealed - consistent with the findings for the p53 levels - the highest fractions of cleaved PARP in the group with the low PEEP ventilation strategy (Figure 8).

Further, the RT-PCR results demonstrated a higher level of expression for genes that are involved in pro-apoptotic mechanisms of cells for the low PEEP ventilated rat groups. APAF1 (29, 37, 64), CDKN1A (7, 27, 28), and GADD45A (7, 66, 88) are p53-inducible genes that are known to be involved in pro-apoptotic mechanisms due to induction by p53. The RT-PCR results for these genes revealed a higher expression in the low PEEP ventilated rat group compared with the “open lung” ventilated group. The results for these genes were statistically significant (Figures 9, 10, 11). These findings indicate a p53-dependent pathway of converting cell damaging physical stimuli in low PEEP ventilation to apoptosis. Further, there were RT-PCR results of the pro-apoptotic but p53-independent genes RBBP7 and RGD1561176 that suggest also a p53-independent apoptosis pathway. Both genes were upregulated in the low PEEP ventilated rat group. In contrast to the results of the p53-inducible genes, the results for the p53-independent genes were not statistically significant (Figures 12, 13).

A reason for anti-apoptotic effects in the high PEEP ventilated rat group may be prevention of the atelectrauma that could damage the lung due to shear stress. Prevention of the atelectrauma leads to activation of cell protective mechanisms leading to decreased gene expression of pro-apoptotic genes. In this way it can be explained that the PCR results are similar in the high PEEP ventilated rat group and the rat group without induced lung injury whereas the low PEEP ventilated rat group where the gene expression of the pro-apoptotic genes is not negatively influenced.

An overview of apoptotic mechanisms is given in Figure 18.

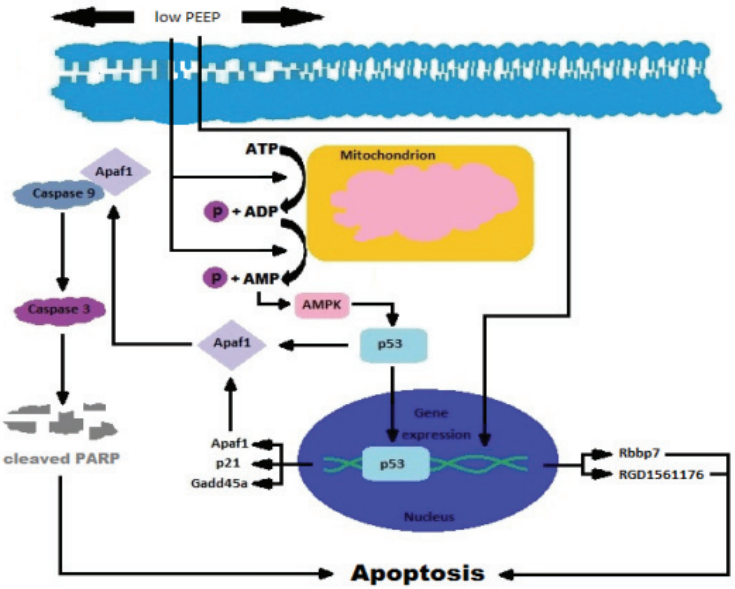

Figure 18: Overview of the pro-apoptotic mechanisms in low PEEP ventilation confirmed by my investigations. ATP: adenosine triphosphate, ADP: adenosine diphosphate, AMP: adenosine monophosphate, P: phosphate.

Taken together, these findings suggest that the "open lung" ventilation strategy in rats promotes cell survival and lung protection. The study presented here, as well as the work of others, reveal that Akt responds to mechanical stimuli, such as those induced by mechanical ventilation, in the lung. It is proposed here that Akt drives the phosphorylation, and thereby inactivation, of GSK3β. This would be protective, since active GSK3β leads to the degradation of β-catenin, which in turn leads to loss of blood-gas barrier integrity (69, 83), a key feature of pulmonary oedema (38). The ability of Akt to promote phosphorylation, and hence, inactivation of GSK3β, would promote the stability of β-catenin, and thus, promote blood-gas barrier integrity. Furthermore, Akt may lead, via a reduction in the AMP:ATP ratio (42), to less phosphorylation of AMPKα (48, 84), leading to inactivation of AMPKα. The apoptosis rate of affected cells would then decrease, because AMPKα promotes cell death (48, 84, 93).

A further mechanism of lung protection is the lower steady-state expression level of p53 in the lungs of "open lung" ventilated rats. Increased steady-state levels of p53, as seen in low PEEP ventilated lungs, leads - via gene regulation - to increased rates of apoptosis in the lungs of the low PEEP ventilated rats. The pro-apoptotic activity of p53 is related to the increased expression of pro-apoptotic p53-inducible genes, the expression of which was increased in the lungs of low PEEP ventilated rats. However, the increased expression of pro-apoptotic p53-independent genes was also noted, indicating that p53-independent pro apoptotic pathways were also operative in the lungs of low PEEP ventilated rats.
Thus, this study revealed the activation of anti-apoptotic pathways, particularly the PI3K-Akt pathway, and inactivation of pro-apoptotic pathways, including p53-dependent and p53-independent mechanisms of apoptosis.

Since it was established that the most harmful effects occur in the low PEEP ventilated rat lungs it was evident to investigate the most affected cells in a most affected lung. The immunohistochemical investigations demonstrated that the cell-injurious stimuli impacted primarily the type I pneumocytes (Figures 14, 15). These cells are in the "front line" in the barrier to the environment, and protect the other lung tissue from harmful physical, chemical, and biological stimuli (52, 99). The reason why type I pneumocytes are primarily affected is not known, however, reasons may include the vastly increased abundance of type I pneumocytes, and the different biological properties and locations of type I pneumocytes when compared with type II pneumocytes. The activation of ERK1/2 noted in this study may also have bearing on the differences observed in the apoptosis of type I pneumocytes versus type II pneumocytes. All injured (i.e. saline lavaged) lungs exhibited an increase in the activation state of ERK1/2, as documented by increased levels of ERK1/2 phosphorylation. Thus, ERK1/2 activation appears to be a general response to injury in saline-lavaged lungs. Activation of ERKs can lead to harmful reactions in the cell, mediated by ROS generation (1, 19, 47). However, ERK1/2 activation may also serve to prevent apoptosis, as has been described for hyperoxic-injury to type II pneumocytes (15). Thus, it may be speculated that ERK1/2-drived pathways operate differently in type I pneumocytes versus type II pneumocytes, which may underlie the differences observed in the apoptosis of type I pneumocytes versus type II pneumocytes. However, no data to support this idea are provided in the studies reported here.

The data presented here make a strong case for the “open lung” ventilation concept as a lung protective ventilation strategy in an intensive care setting. Some of the molecular pathways that may underlie this protective effect of high PEEP ventilation have been revealed, namely, the activation of Akt, which drives anti-apoptotic, and counteracts pro-apoptotic pathways operative in the ventilated, injured lung. Subsequent studies should address whether inhibition of Akt activation in this background may negate the positive effects of Akt activation during high PEEP ventilation of injured lungs, thus validating the Akt pathway as *the* protective pathway induced by high PEEP ventilation.

5. ABSTRACT

The acute respiratory distress syndrome (ARDS) is the major reason for morbidity and mortality in patients treated in intensive care units. Direct or indirect pulmonary injury can lead to ARDS. Mechanical ventilation is the basis of treatment of patients with ARDS. Mechanical ventilation may induce by itself further damage of the lung tissue. To minimise the risk of subsequent ventilator-induced lung injury (VILI), "protective ventilation" strategies were developed. The mechanisms of lung protection due to protective ventilation settings are largely unknown.

The molecular mechanisms of lung protection were examined in lung tissue from a saline lavage ARDS rat model. Rats were divided into three groups: one without induction of lung injury, one with induction of lung injury and low positive end-expiratory pressure (PEEP) ventilation, and one group with induction of lung injury and high PEEP ventilation ("open lung").

From these studies Akt has emerged as a candidate mediator of lung protective pathways during mechanical ventilation of lungs with an "open lung" concept. Akt inhibits the pro-apoptotic factor p53 directly. Further, Akt inactivates AMP-activated protein kinase α (AMPKα) and glycogen synthase kinase 3β (GSK3β). The kinase AMPKα normally activates p53, and thus, Akt can also inhibit p53 indirectly. Active GSK3β leads to a degradation of β-catenin leading to cell membrane instability and apoptosis. This route of apoptosis induction is also subverted by Akt.

That there was a reduced degree of apoptosis under protective "open lung" ventilation was indicated by western blot analyses for the apoptosis marker cleaved poly-ADP-ribose polymerase (PARP), where the amount of cleaved PARP was lowest in the rat group ventilated with the "open lung" strategy. These findings were corroborated by real-time PCR analyses of the pro-apoptotic p53-inducible genes APAF1, CDKN1A and GADD45A, which presented highest expression levels in the low PEEP-ventilated rat group, suggesting p53-dependent apoptotic pathways in VILI. Finally, immunohistochemical examinations revealed that the type I pneumocytes were more affected by apoptosis than type II pneumocytes during mechanical ventilation of the lung.

6. ZUSAMMENFASSUNG

Das akute respiratorische Distress-Syndrom (ARDS) ist der Hauptgrund für Morbidität und Mortalität von auf Intensivstationen behandelten Patienten. ARDS entwickelt sich auf dem Boden einer direkten oder indirekten Schädigung der Lunge. Mechanische Beatmung stellt die Basistherapie von ARDS-Patienten dar. Maschinenbeatmung kann selbst zu weiteren Schädigungen des Lungengewebes führen. Um das Risiko einer entsprechenden beatmungsassoziierten Lungenschädigung (VILI) zu minimieren, wurden lungenschonende Beatmungsstrategien entwickelt. Wie diese Strategien die Lunge schonen, ist größtenteils noch ungeklärt.

Molekulare Mechanismen, die zur Lungenschonung beitragen, wurden in Lungengeweben eines Saline-Lavage ARDS-Rattenmodells untersucht. Die Ratten wurden drei Gruppen zugeteilt: bei einer Gruppe wurde kein ARDS verursacht, bei einer wurde nach ARDS-Auslösung ein niedriger PEEP zur Beatmung gewählt und einer nach ARDS-Provokation eine Beatmung mit hohem PEEP ("open lung") angeboten. Als Dreh- und Angelpunkt anti-apoptotischer Effekte lungenprotektiver Beatmung entpuppte sich Akt. Akt hemmt den pro-apoptotischen Faktor p53 direkt. Darüberhinaus inaktiviert Akt sowohl die AMP-aktivierte Proteinkinase α (AMPKα) als auch die Glycogensynthasekinase 3β (GSK3β). Normalerweise aktiviert AMPKα p53, so dass Akt p53 auch indirekt hemmen kann. Aktive GSK3β führt zum Abbau von β-Catenin, was zur Instabilisierung von Zellmembranen und auch zur Apoptose führt. Dieser Apoptoseweg ist also ebenfalls durch Akt blockiert. Dass unter lungenprotektiver Beatmung tatsächlich weniger Zellen in die Apoptose gehen, zeigten die Western blot-Analysen mit dem Apoptose-Marker poly-ADP-Ribosepolymerase (PARP), bei denen der Anteil von gespaltener PARP in der mit der "open lung"-Strategie beatmeten Rattengruppe am geringsten war. Diese Ergebnisse wurden von real-time PCR-Untersuchungen der pro-apoptotischen, p53-induzierbaren Gene APAF1, CDKN1A und GADD45A gestützt, die die höchsten Expressionslevel in der mit geringem PEEP beatmeten Gruppe zeigten, was einen p53-abhängigen Apoptosesignalweg nahelegt. Schließlich wurde mit immunhistochemischen Untersuchungen gezeigt, dass die Typ I-Alveolarepithelzellen in höherem Maße als die Typ II-Alveolarepithelzellen von Apoptose unter mechanischer Beatmung betroffen sind.

7. ABBREVIATIONS

A

ADP	adenosine diphosphate
ALI	acute lung injury
AMP	adenosine monophosphate
AMPK	AMP-activated protein kinase
Apaf1	apoptotic peptidase activating factor 1
APS	ammonium persulfate
ARDS	acute respiratory distress syndrome
ATP	adenosine triphosphate

B

BAL	bronchoalveolar lavage
BMP	bone morphogenetic protein
BSA	bovine serum albumin

C

cAMP	cyclic adenosine monophosphate
CDKN1A	cyclin-dependent kinase inhibitor 1a
cDNA	complementary DNA
CO_2	carbon dioxide

D

DAG	diacylglycerol
DAPI	4',6-diamidino-2-phenyl-indol
D-MEM	Dulbecco's modification of Eagle's medium
DNA	deoxyribonucleic acid
dNTP	deoxynucleotide triphosphates
dsDNA	double-stranded DNA
DTT	dithiothreitol

E

ECM	extracellular matrix
EDTA	ethylenediaminetetraacetic acid
EGF	epidermal growth factor
EGTA	ethylene glycol tetraacetic acid
ELISA	enzyme-linked immunosorbent assay
eNOS	endothelial nitric oxide synthases
ERK	extracellular signal-related kinase

F

FCS	foetal calf serum
FGF	fibroblast growth factor

G

g	gram or centrifugal force
Gadd	growth arrest and DNA damage
GSK3β	glycogen synthase kinase 3β
GTP	guanosine triphosphate

H

HEPES	4-(2-hydroxyethyl)-1-piperazineethanesulfonic acid
HGF	hepatocyte growth factor
HRPO	horseradish peroxidase
HPRT	hypoxanthine phosphoribosyltransferase

I

IFNγ	interferon γ
IL	interleukin
IP_3	inositol-1,4,5-trisphosphate

J

JNK	c-Jun-NH_2-terminal kinase

K

KGF	keratinocyte growth factor

L

l	liters
LPS	lipopolysaccharide

M

µ	micro
m	milli
MAPK	mitogen-activated protein kinase
MEK	mitogen-activated protein/extracellular signal-related kinase kinase
MKK	mitogen-activated protein kinase kinase
MLC	myosin light chain
mRNA	messenger ribonucleic acid
MSOF	multiple-system organ failure
mTOR	mammalian target of rapamycin

N

NF-κB	nuclear factor-κB
NOS	nitric oxide synthase

P

PARP	poly-ADP-ribose polymerase
PBS	phosphate-buffered saline
PBST	PBS + 0.1 % Tween 20
PCR	polymerase chain reaction
PCWP	pulmonary capillary wedge pressure
PDGF	platelet-derived growth factor
PEEP	positive end-expiratory pressure
PI3K	phosphoinositide 3-kinase
PIP	peak inspiratory pressure
PIP_2	phosphatidylinositol-4,5-bisphosphate

PKA	protein kinase A
PKC	protein kinase C
PLC	phospholipase C
PPAR	peroxisome proliferator-activated receptor
PTK	protein tyrosine kinase

R

Rbbp 7	retinoblastoma binding protein 7
ROCK	Rho-associated kinase
ROS	reactive oxygen species
rpm	revolutions per minute

S

SAPK	stress-activated protein kinase
SDS	sodium dodecyl sulfate
SIRS	systemic inflammatory response syndrome
SP-C	surfactant protein C

T

TEMED	tetramethylethylenediamine
TGFβ	transforming growth factor-β
TNFα	tumour necrosis factor α
Tris	tris(hydroxymethyl)aminomethane

U

UDG	uracil-DNA glycosylase

V

V	volt
VILI	ventilator-induced lung injury

8. REFERENCES

1. Abdulnour RE, Peng X, Finigan JH, Han EJ, Hasan EJ, Birukov KG, Reddy SP, Watkins JE 3rd, Kayyali US, Garcia JG, Tuder RM, Hassoun PM. Mechanical stress activates xanthine oxidoreductase through MAP kinase-dependent pathways. *Am J Physiol Lung Cell Mol Physiol*, 291(3), 345-353 (2006)
2. Ahmad A, Ahmad S, Chang LY, Schaack J, White CW. Endothelial Akt activation by hyperoxia: role in cell survival. *Free Radic Biol Med*, 40(7), 1108-1118 (2006)
3. Albertine KH, Soulier MF, Wang Z, Ishizaka A, Hashimoto S, Zimmerman GA, Matthay MA, Ware LB. Fas and fas ligand are up-regulated in pulmonary edema fluid and lung tissue of patients with acute lung injury and the acute respiratory distress syndrome. *Am J Pathol*, 161(5), 1783-1796 (2002)
4. Amato MB, Barbas CS, Medeiros DM, Magaldi RB, Schettino GP, Lorenzi-Filho G, Kairalla RA, Deheinzelin D, Munoz C, Oliveira R, Takagaki TY, Carvalho CR. Effect of a protective-ventilation strategy on mortality in the acute respiratory distress syndrome. *N Engl J Med*, 338(6), 347-354 (1998)
5. Amato MB, Barbas CS, Medeiros DM, Schettino Gde P, Lorenzi Filho G, Kairalla RA, Deheinzelin D, Morais C, Fernandes Ede O, Takagaki TY, et al. Beneficial effects of the "open lung approach" with low distending pressures in acute respiratory distress syndrome. A prospective randomized study on mechanical ventilation. *Am J Respir Crit Care Med*, 152(6 Pt 1), 1835-1846 (1995)
6. Artigas A, Bernard GR, Carlet J, Dreyfuss D, Gattinoni L, Hudson L, Lamy M, Marini JJ, Matthay MA, Pinsky MR, Spragg R, Suter PM. The American-European Consensus Conference on ARDS, part 2: Ventilatory, pharmacologic, supportive therapy, study design strategies, and issues related to recovery and remodeling. Acute respiratory distress syndrome. *Am J Respir Crit Care Med*, 157(4 Pt 1), 1332-1347 (1998)

7. Baldi A, De Luca A, Esposito V, Campioni M, Spugnini EP, Citro G. Tumor suppressors and cell-cycle proteins in lung cancer. *Patholog Res Int*, 605042 (2011)

8. Bao S, Wang Y, Sweeney P, Chaudhuri A, Doseff AI, Marsh CB, Knoell DL. Keratinocyte growth factor induces Akt kinase activity and inhibits Fas-mediated apoptosis in A549 lung epithelial cells. *Am J Physiol Lung Cell Mol Physiol*, 288(1), 36-42 (2005)

9. Barbas CS, de Matos GF, Pincelli MP, da Rosa Borges E, Antunes T, de Barros JM, Okamoto V, Borges JB, Amato MB, de Carvalho CR. Mechanical ventilation in acute respiratory failure: recruitment and high positive end-expiratory pressure are necessary. *Curr Opin Crit Care*, 11(1), 18-28 (2005)

10. Bernard GR, Artigas A, Brigham KL, Carlet J, Falke K, Hudson L, Lamy M, LeGall JR, Morris A, Spragg R. Report of the American-European Consensus conference on acute respiratory distress syndrome: definitions, mechanisms, relevant outcomes, and clinical trial coordination. Consensus Committee. *J Crit Care*, 9(1), 72-81 (1994)

11. Bernard GR. Acute respiratory distress syndrome: a historical perspective. *Am J Respir Crit Care Med*, 172(7), 798-806 (2005)

12. Billottet C, Elkhatib N, Thiery JP, Jouanneau J. Targets of fibroblast growth factor 1 (FGF-1) and FGF-2 signaling involved in the invasive and tumorigenic behavior of carcinoma cells. *Mol Biol Cell*, 15(10), 4725-4734 (2004)

13. Birukova AA, Birukov KG, Adyshev D, Usatyuk P, Natarajan V, Garcia JG, Verin AD. Involvement of microtubules and Rho pathway in TGF-beta1-induced lung vascular barrier dysfunction. *J Cell Physiol*, 204(3), 934-947 (2005)

14. Brower RG, Lanken PN, MacIntyre N, Matthay MA, Morris A, Ancukiewicz M, Schoenfeld D, Thompson BT; National Heart, Lung, and Blood Institute ARDS Clinical Trials Network. Higher versus lower positive end-expiratory pressures in patients with the acute respiratory distress syndrome. *N Engl J Med*, 351(4), 327-336 (2004)

15. Buckley S, Driscoll B, Barsky L, Weinberg K, Anderson K, Warburton D. ERK activation protects against DNA damage and apoptosis in hyperoxic rat AEC2. *Am J Physiol*, 277(1 Pt 1), 159-166 (1999)
16. Budinger GR, Chandel NS, Donnelly HK, Eisenbart J, Oberoi M, Jain M. Active transforming growth factor-beta1 activates the procollagen I promoter in patients with acute lung injury. *Intensive Care Med*, 31(1), 121-128 (2005)
17. Cao H, Dronadula N, Rao GN. Thrombin induces expression of FGF-2 via activation of PI3K-Akt-Fra-1 signaling axis leading to DNA synthesis and motility in vascular smooth muscle cells. *Am J Physiol Cell Physiol*, 290(1), 172-182 (2006)
18. Chang L, Karin M. Mammalian MAP kinase signalling cascades. *Nature*, 410(6824), 37-40 (2001)
19. Chapman KE, Sinclair SE, Zhuang D, Hassid A, Desai LP, Waters CM. Cyclic mechanical strain increases reactive oxygen species production in pulmonary epithelial cells. *Am J Physiol Lung Cell Mol Physiol*, 289(5), 834-841 (2005)
20. Chicurel ME, Chen CS, Ingber DE. Cellular control lies in the balance of forces. *Curr Opin Cell Biol*, 10(2), 232-239 (1998)
21. Choi WI, Quinn DA, Park KM, Moufarrej RK, Jafari B, Syrkina O, Bonventre JV, Hales CA. Systemic microvascular leak in an in vivo rat model of ventilator-induced lung injury. *Am J Respir Crit Care Med*, 167(12), 1627-1632 (2003)
22. Correa-Meyer E, Pesce L, Guerrero C, Sznajder JI. Cyclic stretch activates ERK1/2 via G proteins and EGFR in alveolar epithelial cells. *Am J Physiol Lung Cell Mol Physiol*, 282(5), 883-891 (2002)
23. Coulter KR, Doseff A, Sweeney P, Wang Y, Marsh CB, Wewers MD, Knoell DL. Opposing effect by cytokines on Fas-mediated apoptosis in A549 lung epithelial cells. *Am J Respir Cell Mol Biol*, 26(1), 58-66 (2002)
24. Crosby LM, Waters CM. Epithelial repair mechanisms in the lung. *Am J Physiol Lung Cell Mol Physiol*, 298(6), 715-731 (2010)
25. Cuschieri J, Maier RV. Mitogen-activated protein kinase (MAPK). *Crit Care Med*, 33(12 Suppl), 417-419 (2005)

26. Cuzzocrea S, Crisafulli C, Mazzon E, Esposito E, Muià C, Abdelrahman M, Di Paola R, Thiemermann C. Inhibition of glycogen synthase kinase-3beta attenuates the development of carrageenan-induced lung injury in mice. *Br J Pharmacol*, 149(6), 687-702 (2006)

27. Das S, Boswell SA, Aaronson SA, Lee SW. P53 promoter selection: choosing between life and death. *Cell Cycle*, 7(2), 154-157 (2008)

28. Das S, Raj L, Zhao B, Kimura Y, Bernstein A, Aaronson SA, Lee SW. Hzf Determines cell survival upon genotoxic stress by modulating p53 transactivation. *Cell*, 130(4), 624-637 (2007)

29. Deng WG, Kawashima H, Wu G, Jayachandran G, Xu K, Minna JD, Roth JA, Ji L. Synergistic tumor suppression by coexpression of FUS1 and p53 is associated with down-regulation of murine double minute-2 and activation of the apoptotic protease-activating factor 1-dependent apoptotic pathway in human non-small cell lung cancer cells. *Cancer Res*, 67(2), 709-717 (2007)

30. Derynck R, Zhang YE. Smad-dependent and Smad-independent pathways in TGF-beta family signalling. *Nature*, 425(6958), 577-584 (2003)

31. Dolinay T, Kaminski N, Felgendreher M, Kim HP, Reynolds P, Watkins SC, Karp D, Uhlig S, Choi AM. Gene expression profiling of target genes in ventilator-induced lung injury. *Physiol Genomics*, 26(1), 68-75 (2006)

32. Dolinay T, Wu W, Kaminski N, Ifedigbo E, Kaynar AM, Szilasi M, Watkins SC, Ryter SW, Hoetzel A, Choi AM. Mitogen-activated protein kinases regulate susceptibility to ventilator-induced lung injury. *PLoS One*, 3(2), e1601 (2008)

33. Dos Santos CC, Slutsky AS. Invited review: mechanisms of ventilator-induced lung injury: a perspective. *J Appl Physiol*, 89(4), 1645-1655 (2000)

34. Dreyfuss D, Saumon G. Ventilator-induced lung injury: lessons from experimental studies. *Am J Respir Crit Care Med*, 157(1), 294-323 (1998)

35. Fahy RJ, Lichtenberger F, McKeegan CB, Nuovo GJ, Marsh CB, Wewers MD. The acute respiratory distress syndrome: a role for transforming growth factor-beta 1. *Am J Respir Cell Mol Biol*, 28(4), 499-503 (2003)

36. Fan E, Needham DM, Stewart TE. Ventilatory management of acute lung injury and acute respiratory distress syndrome. *JAMA*, 294(22), 2889-2896 (2005)

37. Fortin A, Cregan SP, MacLaurin JG, Kushwaha N, Hickman ES, Thompson CS, Hakim A, Albert PR, Cecconi F, Helin K, Park DS, Slack RS. APAF1 is a key transcriptional target for p53 in the regulation of neuronal cell death. *J Cell Biol*, 155(2), 207-216 (2001)

38. Frank JA, Matthay MA. Science review: mechanisms of ventilator-induced injury. *Crit Care*, 7(3), 233-241 (2003)

39. Gattinoni L, Bombino M, Pelosi P, Lissoni A, Pesenti A, Fumagalli R, Tagliabue M. Lung structure and function in different stages of severe adult respiratory distress syndrome. *JAMA*, 271(22), 1772-1779 (1994)

40. Girard TD, Bernard GR. Mechanical ventilation in ARDS: a state-of-the-art review. *Chest*, 131(3), 921-929 (2007)

41. Gnecchi M, He H, Noiseux N, Liang OD, Zhang L, Morello F, Mu H, Melo LG, Pratt RE, Ingwall JS, Dzau VJ. Evidence supporting paracrine hypothesis for Akt-modified mesenchymal stem cell-mediated cardiac protection and functional improvement. *FASEB J*, 20(6), 661-669 (2006)

42. Gottlob K, Majewski N, Kennedy S, Kandel E, Robey RB, Hay N. Inhibition of early apoptotic events by Akt/PKB is dependent on the first committed step of glycolysis and mitochondrial hexokinase. *Genes Dev*, 15(11), 1406-1418 (2001)

43. Halbertsma FJ, Vaneker M, Scheffer GJ, van der Hoeven JG. Cytokines and biotrauma in ventilator-induced lung injury: a critical review of the literature. *Neth J Med*, 63(10), 382-392 (2005)

44. Halter JM, Steinberg JM, Gatto LA, DiRocco JD, Pavone LA, Schiller HJ, Albert S, Lee HM, Carney D, Nieman GF. Effect of positive end-expiratory pressure and tidal volume on lung injury induced by alveolar instability. *Crit Care*, 11(1), R20 (2007)

45. Hammerschmidt S, Kuhn H, Gessner C, Seyfarth HJ, Wirtz H. Stretch-induced alveolar type II cell apoptosis: role of endogenous bradykinin and PI3K-Akt signaling. *Am J Respir Cell Mol Biol*, 37(6), 699-705 (2007)

46. Hammerschmidt S, Kuhn H, Grasenack T, Gessner C, Wirtz H. Apoptosis and necrosis induced by cyclic mechanical stretching in alveolar type II cells. *Am J Respir Cell Mol Biol*, 30(3), 396-402 (2004)

47. Han SI, Kim YS, Kim TH. Role of apoptotic and necrotic cell death under physiologic conditions. *BMB Rep*, 41(1), 1-10 (2008)

48. Hardie DG, Hawley SA, Scott JW. AMP-activated protein kinase--development of the energy sensor concept. *J Physiol*, 574(Pt 1), 7-15 (2006)

49. Hashimoto S, Kobayashi A, Kooguchi K, Kitamura Y, Onodera H, Nakajima H. Upregulation of two death pathways of perforin/granzyme and FasL/Fas in septic acute respiratory distress syndrome. *Am J Respir Crit Care Med*, 161(1), 237-243 (2000)

50. Herold G. Adult Respiratory Distress Syndrome. In: Herold G (Hrsg.). Innere Medizin. Köln. 316-317 (2009)

51. Herold G. Herzinsuffizienz. In: Herold G (Hrsg.). Innere Medizin. Köln. 190-198 (2009)

52. Herzog EL, Brody AR, Colby TV, Mason R, Williams MC. Knowns and unknowns of the alveolus. *Proc Am Thorac Soc*, 5(7), 778-782 (2008)

53. Imanaka H, Shimaoka M, Matsuura N, Nishimura M, Ohta N, Kiyono H. Ventilator-induced lung injury is associated with neutrophil infiltration, macrophage activation, and TGF-beta 1 mRNA upregulation in rat lungs. *Anesth Analg*, 92(2), 428-436 (2001)

54. International consensus conferences in intensive care medicine: Ventilator-associated Lung Injury in ARDS. *Am J Respir Crit Care Med*, 160(6), 2118-2124 (1999)

55. Kaplan JM, Hake PW, Denenberg A, Nowell M, Piraino G, Zingarelli B. Phosphorylation of extracellular signal-regulated kinase (ERK)-1/2 Is associated with the downregulation of peroxisome proliferator-activated receptor (PPAR)-γ during polymicrobial sepsis. *Mol Med*, 16(11-12), 491-497 (2010)

56. Kitamura Y, Hashimoto S, Mizuta N, Kobayashi A, Kooguchi K, Fujiwara I, Nakajima H. Fas/FasL-dependent apoptosis of alveolar cells after lipopolysaccharide-induced lung injury in mice. *Am J Respir Crit Care Med*, 163(3 Pt 1), 762-769 (2001)

57. Kloot TE, Blanch L, Melynne Youngblood A, Weinert C, Adams AB, Marini JJ, Shapiro RS, Nahum A. Recruitment maneuvers in three experimental models of acute lung injury. Effect on lung volume and gas exchange. *Am J Respir Crit Care Med*, 161(5), 1485-1494 (2000)

58. Krebs J, Pelosi P, Tsagogiorgas C, Zoeller L, Rocco PR, Yard B, Luecke T. Open lung approach associated with high-frequency oscillatory or low tidal volume mechanical ventilation improves respiratory function and minimizes lung injury in healthy and injured rats. *Crit Care*, 14(5), R183 (2010)

59. Kwong J, Hong L, Liao R, Deng Q, Han J, Sun P. p38alpha and p38gamma mediate oncogenic ras-induced senescence through differential mechanisms. *J Biol Chem*, 284(17), 11237-11246 (2009)

60. Lachmann B, Robertson B, Vogel J. In vivo lung lavage as an experimental model of the respiratory distress syndrome. *Acta Anaesthesiol Scand*, 24(3), 231-236 (1980)

61. Lee YH, Suzuki YJ, Griffin AJ, Day RM. Hepatocyte growth factor regulates cyclooxygenase-2 expression via beta-catenin, Akt, and p42/p44 MAPK in human bronchial epithelial cells. *Am J Physiol Lung Cell Mol Physiol*, 294(4), 778-786 (2008)

62. Lewandowski K, Lewandowski M. Epidemiology of ARDS. *Minerva Anestesiol*, 72(6), 473-477 (2006)

63. Li LF, Liao SK, Lee CH, Huang CC, Quinn DA. Involvement of Akt and endothelial nitric oxide synthase in ventilation-induced neutrophil infiltration: a prospective, controlled animal experiment. *Crit Care*, 11(4), R89 (2007)

64. Li P, Nijhawan D, Budihardjo I, Srinivasula SM, Ahmad M, Alnemri ES, Wang X. Cytochrome c and dATP-dependent formation of Apaf-1/caspase-9 complex initiates an apoptotic protease cascade. *Cell*, 91(4), 479-489 (1997)

65. Liang J, Slingerland JM. Multiple roles of the PI3K/PKB (Akt) pathway in cell cycle progression. *Cell Cycle*, 2(4), 339-345 (2003)

66. Liebermann DA, Hoffman B. Gadd45 in stress signaling. *J Mol Signal*, 3, 15 (2008)

67. Liebler JM, Qu Z, Buckner B, Powers MR, Rosenbaum JT. Fibroproliferation and mast cells in the acute respiratory distress syndrome. *Thorax*, 53(10), 823-829 (1998)

68. Lin WC, Lin CF, Chen CL, Chen CW, Lin YS. Prediction of outcome in patients with acute respiratory distress syndrome by bronchoalveolar lavage inflammatory mediators. *Exp Biol Med (Maywood)*, 235(1), 57-65 (2010)

69. Liu F, Schaphorst KL, Verin AD, Jacobs K, Birukova A, Day RM, Bogatcheva N, Bottaro DP, Garcia JG. Hepatocyte growth factor enhances endothelial cell barrier function and cortical cytoskeletal rearrangement: potential role of glycogen synthase kinase-3beta. *FASEB J*, 16(9), 950-962 (2002)

70. Liu M, Tanswell AK, Post M. Mechanical force-induced signal transduction in lung cells. *Am J Physiol*, 277(4 Pt 1), 667-683 (1999)

71. Lu Q, Harrington EO, Rounds S. Apoptosis and lung injury. *Keio J Med*, 54(4), 184-189 (2005)

72. Lu S, Ren C, Liu Y, Epner DE. PI3K-Akt signaling is involved in the regulation of p21(WAF/CIP) expression and androgen-independent growth in prostate cancer cells. *Int J Oncol*, 28(1), 245-251 (2006)

73. Luecke T, Meinhardt JP, Herrmann P, Weiss A, Quintel M, Pelosi P. Oleic acid vs saline solution lung lavage-induced acute lung injury: effects on lung morphology, pressure-volume relationships, and response to positive end-expiratory pressure. *Chest*, 130(2), 392-401 (2006)

74. Luecke T, Roth H, Herrmann P, Joachim A, Weisser G, Pelosi P, Quintel M. PEEP decreases atelectasis and extravascular lung water but not lung tissue volume in surfactant-washout lung injury. *Intensive Care Med*, 29(11), 2026-2033 (2003)

75. Luhr OR, Antonsen K, Karlsson M, Aardal S, Thorsteinsson A, Frostell CG, Bonde J. Incidence and mortality after acute respiratory failure and acute respiratory distress syndrome in Sweden, Denmark, and Iceland. The ARF Study Group. *Am J Respir Crit Care Med*, 159(6), 1849-1861 (1999)

76. Luo HR, Hattori H, Hossain MA, Hester L, Huang Y, Lee-Kwon W, Donowitz M, Nagata E, Snyder SH. Akt as a mediator of cell death. *Proc Natl Acad Sci U S A*, 100(20), 11712-11717 (2003)

77. Martin TR, Hagimoto N, Nakamura M, Matute-Bello G. Apoptosis and epithelial injury in the lungs. *Proc Am Thorac Soc*, 2(3), 214-220 (2005)

78. Martin TR. Interactions between mechanical and biological processes in acute lung injury. *Proc Am Thorac Soc*, 5(3), 291-296 (2008)

79. Meade MO, Cook DJ, Guyatt GH, Slutsky AS, Arabi YM, Cooper DJ, Davies AR, Hand LE, Zhou Q, Thabane L, Austin P, Lapinsky S, Baxter A, Russell J, Skrobik Y, Ronco JJ, Stewart TE; Lung Open Ventilation Study Investigators. Ventilation strategy using low tidal volumes, recruitment maneuvers, and high positive end-expiratory pressure for acute lung injury and acute respiratory distress syndrome: a randomized controlled trial. *JAMA*, 299(6), 637-645 (2008)

80. Meyer NJ, Huang Y, Singleton PA, Sammani S, Moitra J, Evenoski CL, Husain AN, Mitra S, Moreno-Vinasco L, Jacobson JR, Lussier YA, Garcia JG. GADD45a is a novel candidate gene in inflammatory lung injury via influences on Akt signaling. *FASEB J*, 23(5), 1325-1337 (2009)

81. Meyrick B. Pathology of the adult respiratory distress syndrome. *Crit Care Clin*, 2(3), 405-428 (1986)

82. Mitsuuchi Y, Johnson SW, Selvakumaran M, Williams SJ, Hamilton TC, Testa JR. The phosphatidylinositol 3-kinase/AKT signal transduction pathway plays a critical role in the expression of $p21^{WAF1/CIP1/SDI1}$ induced by cisplatin and paclitaxel. *Cancer Res*, 60(19), 5390-5394 (2000)

83. Miyahara T, Hamanaka K, Weber DS, Drake DA, Anghelescu M, Parker JC. Phosphoinositide 3-kinase, Src, and Akt modulate acute ventilation-induced vascular permeability increases in mouse lungs. *Am J Physiol Lung Cell Mol Physiol*, 293(1), 11-21 (2007)

84. Motoshima H, Goldstein BJ, Igata M, Araki E. AMPK and cell proliferation - AMPK as a therapeutic target for atherosclerosis and cancer. *J Physiol*, 574(Pt1), 63-71 (2006)

85. Nakamura T, Mizuno S. The discovery of hepatocyte growth factor (HGF) and its significance for cell biology, life sciences and clinical medicine. *Proc Jpn Acad Ser B Phys Biol Sci*, 86(6), 588-610 (2010)

86. Neumann P, Berglund JE, Fernández Mondéjar E, Magnusson A, Hedenstierna G. Dynamics of lung collapse and recruitment during prolonged breathing in porcine lung injury. *J Appl Physiol*, 85(4), 1533-1543 (1998)

87. Ning QM, Wang XR. Activations of mitogen-activated protein kinase and nuclear factor-kappaB by mechanical stretch result in ventilation-induced lung injury. *Med Hypotheses*, 68(2), 356-360 (2007)

88. O'Reilly MA, Staversky RJ, Watkins RH, Maniscalco WM, Keng PC. p53-independent induction of GADD45 and GADD153 in mouse lungs exposed to hyperoxia. *Am J Physiol Lung Cell Mol Physiol*, 278(3), 552-559 (2000)

89. Oudin S, Pugin J. Role of MAP kinase activation in interleukin-8 production by human BEAS-2B bronchial epithelial cells submitted to cyclic stretch. *Am J Respir Cell Mol Biol*, 27(1), 107-114 (2002)

90. Papadakos PJ, Lachmann B. The open lung concept of alveolar recruitment can improve outcome in respiratory failure and ARDS. *Mt Sinai J Med*, 69(1-2), 73-77 (2002)

91. Pavone LA, Albert S, Carney D, Gatto LA, Halter JM, Nieman GF. Injurious mechanical ventilation in the normal lung causes a progressive pathologic change in dynamic alveolar mechanics. *Crit Care*, 11(3), R64 (2007)

92. Perl M, Chung CS, Perl U, Lomas-Neira J, de Paepe M, Cioffi WG, Ayala A. Fas-induced pulmonary apoptosis and inflammation during indirect acute lung injury. *Am J Respir Crit Care Med*, 176(6), 591-601 (2007)

93. Pietsch EC, Sykes SM, McMahon SB, Murphy ME. The p53 family and programmed cell death. *Oncogene*, 27(50), 6507-6521 (2008)

94. Portnoy J, Curran-Everett D, Mason RJ. Keratinocyte growth factor stimulates alveolar type II cell proliferation through the extracellular signal-regulated kinase and phosphatidylinositol 3-OH kinase pathways. *Am J Respir Cell Mol Biol*, 30(6), 901-907 (2004)

95. Qiao R, Yan W, Clavijo C, Mehrian-Shai R, Zhong Q, Kim KJ, Ann D, Crandall ED, Borok Z. Effects of KGF on alveolar epithelial cell transdifferentiation are mediated by JNK signaling. *Am J Respir Cell Mol Biol*, 38(2), 239-246 (2008)

96. Ricard JD, Dreyfuss D, Saumon G. Ventilator-induced lung injury. *Eur Respir J Suppl*, 42, 2-9 (2003)

97. Rosenthal C, Caronia C, Quinn C, Lugo N, Sagy M. A comparison among animal models of acute lung injury. *Crit Care Med*, 26(5), 912-916 (1998)

98. Rubenfeld GD, Herridge MS. Epidemiology and outcomes of acute lung injury. *Chest*, 131(2), 554-562 (2007)

99. Schiebler TH, Schmidt W. Atmungsorgane. In: Schiebler TH, Schmidt W (Hrsg.). Anatomie. Springer, Heidelberg. 489-506 (2003)

100. Schönherr E, Levkau B, Schaefer L, Kresse H, Walsh K. Decorin-mediated signal transduction in endothelial cells. Involvement of Akt/protein kinase B in up-regulation of p21(WAF1/CIP1) but not p27(KIP1). *J Biol Chem*, 276(44), 40687-40692 (2001)

101. Sharon H, Amar D, Levdansky E, Mircus G, Shadkchan Y, Shamir R, Osherov N. PrtT-regulated proteins secreted by Aspergillus fumigatus activate MAPK signaling in exposed A549 lung cells leading to necrotic cell death. *PLoS One*, 6(3), e17509 (2011)

102. Slutsky AS. Lung injury caused by mechanical ventilation. *Chest*, 116(1), 9-15 (1999)

103. Striebel HW. Beatmungstherapie. In: Striebel HW. Anästhesie – Intensivmedizin – Notfallmedizin. Schattauer, Stuttgart. 330-362 (2006)

104. Takeuchi M, Goddon S, Dolhnikoff M, Shimaoka M, Hess D, Amato MB, Kacmarek RM. Set positive end-expiratory pressure during protective ventilation affects lung injury. *Anesthesiology*, 97(3), 682-692 (2002)

105. The Acute Respiratory Distress Syndrome Network. Ventilation with lower tidal volumes as compared with traditional tidal volumes for acute lung injury and the acute respiratory distress syndrome. *N Engl J Med*, 342(18), 1301-1308 (2000)

106. Thews G, Thews O. Lungenatmung. In: Schmidt RF, Lang F (Hrsg.). Physiologie des Menschen mit Pathophysiologie. Springer, Heidelberg. 755-785 (2007)

107. Thornton TM, Pedraza-Alva G, Deng B, Wood CD, Aronshtam A, Clements JL, Sabio G, Davis RJ, Matthews DE, Doble B, Rincon M. Phosphorylation by p38 MAPK as an alternative pathway for GSK3beta inactivation. *Science*, 320(5876), 667-670 (2008)

108. Toker A. Protein kinases as mediators of phosphoinositide 3-kinase signaling. *Mol Pharmacol*, 57(4), 652-658 (2000)

109. Tomashefski JF Jr. Pulmonary pathology of acute respiratory distress syndrome. *Clin Chest Med*, 21(3), 435-466 (2000)

110. Tremblay L, Valenza F, Ribeiro SP, Li J, Slutsky AS. Injurious ventilatory strategies increase cytokines and c-fos m-RNA expression in an isolated rat lung model. *J Clin Invest*, 99(5), 944-952 (1997)

111. Tront JS, Huang Y, Fornace AJ Jr, Hoffman B, Liebermann DA. Gadd45a functions as a promoter or suppressor of breast cancer dependent on the oncogenic stress. *Cancer Res*, 70(23), 9671-9681 (2010)

112. Tschumperlin DJ, Dai G, Maly IV, Kikuchi T, Laiho LH, McVittie AK, Haley KJ, Lilly CM, So PT, Lauffenburger DA, Kamm RD, Drazen JM. Mechanotransduction through growth-factor shedding into the extracellular space. *Nature*, 429(6987), 83-86 (2004)

113. Tsubaki M, Yamazoe Y, Yanae M, Satou T, Itoh T, Kaneko J, Kidera Y, Moriyama K, Nishida S. Blockade of the Ras/MEK/ERK and Ras/PI3K/Akt pathways by statins reduces the expression of bFGF, HGF, and TGF-β as angiogenic factors in mouse osteosarcoma. *Cytokine*, 54(1), 100-107 (2011)

114. Uhlig S. Ventilation-induced lung injury and mechanotransduction: stretching it too far? *Am J Physiol Lung Cell Mol Physiol*, 282(5), 892-896 (2002)

115. Uhlig U, Haitsma JJ, Goldmann T, Poelma DL, Lachmann B, Uhlig S. Ventilation-induced activation of the mitogen-activated protein kinase pathway. *Eur Respir J*, 20(4), 946-956 (2002)

116. Undevia NS, Dorscheid DR, Marroquin BA, Gugliotta WL, Tse R, White SR. Smad and p38-MAPK signaling mediates apoptotic effects of transforming growth factor-beta1 in human airway epithelial cells. *Am J Physiol Lung Cell Mol Physiol*, 287(3), 515-524 (2004)

117. Van Aelst L, D'Souza-Schorey C. Rho GTPases and signaling networks. *Genes Dev*, 11(18), 2295-2322 (1997)

118. Vlahakis NE, Hubmayr RD. Cellular stress failure in ventilator-injured lungs. *Am J Respir Crit Care Med*, 171(12), 1328-1342 (2005)

119. Vlahakis NE, Hubmayr RD. Response of alveolar cells to mechanical stress. *Curr Opin Crit Care*, 9(1), 2-8 (2003)

120. Wang S, Zhang Z, Lin X, Xu DS, Feng Y, Ding K. A polysaccharide, MDG-1, induces S1P1 and bFGF expression and augments survival and angiogenesis in the ischemic heart. *Glycobiology*, 20(4), 473-484 (2010)

121. Wharton K, Derynck R. TGFbeta family signaling: novel insights in development and disease. *Development*, 136(22), 3691-3697 (2009)

122. Whitehead T, Slutsky AS. The pulmonary physician in critical care • 7: ventilator induced lung injury. *Thorax*, 57(7), 635-642 (2002)

123. Wirtz HR, Dobbs LG. The effects of mechanical forces on lung functions. *Respir Physiol*, 119(1), 1-17 (2000)

124. Yohn NL, Bingaman CN, DuMont AL, Yoo LI. Phosphatidylinositol 3'-kinase, mTOR, and glycogen synthase kinase-3β mediated regulation of p21 in human urothelial carcinoma cells. *BMC Urol*, 11-19 (2011)

125. Yum HK, Arcaroli J, Kupfner J, Shenkar R, Penninger JM, Sasaki T, Yang KY, Park JS, Abraham E. Involvement of phosphoinositide 3-kinases in neutrophil activation and the development of acute lung injury. *J Immunol*, 167(11), 6601-6608 (2001)

126. Zambon M, Vincent JL. Mortality rates for patients with acute lung injury/ARDS have decreased over time. *Chest*, 133(5), 1120-1127 (2008)

127. Zhang B, Cao H, Rao GN. Fibroblast growth factor-2 is a downstream mediator of phosphatidylinositol 3-kinase-Akt signaling in 14,15-epoxyeicosatrienoic acid-induced angiogenesis. *J Biol Chem*, 281(2), 905-914 (2006)

9. ERKLÄRUNG ZUR DISSERTATION

„Hiermit erkläre ich, dass ich die vorliegende Arbeit selbständig und ohne unzulässige Hilfe oder Benutzung anderer als der angegebenen Hilfsmittel angefertigt habe. Alle Textstellen, die wörtlich oder sinngemäß aus veröffentlichten oder nichtveröffentlichten Schriften entnommen sind, und alle Angaben, die auf mündlichen Auskünften beruhen, sind als solche kenntlich gemacht. Bei den von mir durchgeführten und in der Dissertation erwähnten Untersuchungen habe ich die Grundsätze guter wissenschaftlicher Praxis, wie sie in der „Satzung der Justus-Liebig-Universität Gießen zur Sicherung guter wissenschaftlicher Praxis“ niedergelegt sind, eingehalten sowie ethische, datenschutzrechtliche und tierschutzrechtliche Grundsätze befolgt. Ich versichere, dass Dritte von mir weder unmittelbar noch mittelbar geldwerte Leistungen für Arbeiten erhalten haben, die im Zusammenhang mit dem Inhalt der vorgelegten Dissertation stehen, oder habe diese nachstehend spezifiziert. Die vorgelegte Arbeit wurde weder im Inland noch im Ausland in gleicher oder ähnlicher Form einer anderen Prüfungsbehörde zum Zweck einer Promotion oder eines anderen Prüfungsverfahrens vorgelegt. Alles aus anderen Quellen und von anderen Personen übernommene Material, das in der Arbeit verwendet wurde oder auf das direkt Bezug genommen wird, wurde als solches kenntlich gemacht. Insbesondere wurden alle Personen genannt, die direkt und indirekt an der Entstehung der vorliegenden Arbeit beteiligt waren. Mit der Überprüfung meiner Arbeit durch eine Plagiatserkennungssoftware bzw. ein internetbasiertes Softwareprogramm erkläre ich mich einverstanden.“

Gießen, 14.05.2013 Sven Fuest

10. DANKSAGUNG

An dieser Stelle möchte ich allen danken, die zu der vorliegenden Arbeit beigetragen haben.

Insbesondere gilt der Dank Herrn Dr. Rory Morty für die Möglichkeit der Promotion, der Überlassung des Themas sowie die engagierte Unterstützung während der Durchführung der Arbeit.

Darüberhinaus möchte ich allen Mitgliedern der AGs Eickelberg und Morty – insbesondere Simone Becker - für die gute Einarbeitung und die jederzeit gewährte Hilfe und Unterstützung bei den Experimenten danken. Zudem danke ich den Mitarbeitern der Erasmus-Universität Rotterdam, insbesondere Herrn MD Irwin Reiss, für die Durchführung der Versuche am Tier sowie für die Präparation und Überlassung der Rattenlungen.

Familie und Freunden sei für die langjährige Unterstützung in Studium und während der Anfertigung der Dissertation gedankt.

www.lehmanns.de

This thesis evaluates molecular mechanisms involved in acute respiratory distress syndrome and ventilator-induced lung injury. Open-lung ventilation strategies are known to be lung protective. Different molecular biological and immunohistochemical research methods provided discoveries in the lung protective mechanisms induced by open-lung ventilation strategies. The thesis illustrates these scientific findings imbedded in detailed description of the used research methods and basic as well as up-to-date knowledge of acute respiratory distress syndrome, ventilator-induced lung injury, and cell death mechanisms. Coloured figures facilitate the understanding of the findings.

ISBN: 978-3-86541-610-0

9 783865 416100

lehmanns media